Fisheries New Zealand
Tini a Tangaroa

Acoustic estimates of southern blue whiting from the Campbell Island Rise, August–September 2016 (TAN1610)

New Zealand Fisheries Assessment Report 2018/56

R.L. O'Driscoll
K. Large
P. Marriott

ISSN 1179-5352 (online)
ISBN 978-1-98-857138-6 (online)

December 2018

New Zealand Government

Requests for further copies should be directed to:

Publications Logistics Officer
Ministry for Primary Industries
PO Box 2526
WELLINGTON 6140

Email: brand@mpi.govt.nz
Telephone: 0800 00 83 33
Facsimile: 04-894 0300

This publication is also available on the Ministry for Primary Industries websites at:
http://www.mpi.govt.nz/news-and-resources/publications
http://fs.fish.govt.nz go to Document library/Research reports

TABLE OF CONTENTS

EXECUTIVE SUMMARY

O'Driscoll, R.L.; Large, K.; Marriott, P. (2018). Acoustic estimates of southern blue whiting from the Campbell Island Rise, August–September 2016 (TAN1610).

***New Zealand Fisheries Assessment Report 2018/56* 60 p.**

The 12th acoustic survey of southern blue whiting (SBW) on the Campbell Island Rise was carried out from 26 August to 23 September 2016 (TAN1610). Two snapshots of the survey area were completed: on 31 August – 10 September and 10–20 September respectively. Nineteen bottom trawls and one midwater trawl were carried out during the survey to collect data on species composition, length frequency, and spawning state of SBW. Lowered and moored video cameras were deployed on five occasions to measure the tilt angle distribution of SBW *in situ*.

Three aggregations of adult SBW were detected during the survey. Pre-spawning adult SBW were detected in the north (strata 2 and 4) and south (stratum 7S) of the survey area during snapshot 1, but no strong marks were detected in the east. Stratum boundaries were modified in snapshot 2, with some strata extended and others reduced, in an attempt to better reflect the distribution of fish. Gonad stage data from the commercial fleet suggested that the first spawning occurred during snapshot 1 from 1–8 September. During snapshot 2, a large post-spawning aggregation was found in the eastern area (centred in stratum 8S, but extending into strata 6S and 8E). Spawning and post-spawning adult SBW were also observed in the south (stratum 7S) and north (strata 2, 4, and 5) during the second snapshot. The second spawning occurred from 18–25 September.

Immature southern blue whiting marks were widespread at depths from 370–410 m in strata 2, 4, 5, 7N, and 7S. These were fish with lengths between 25 and 30 cm and were probably 2 or 3 years old (2014 or 2013 year-class). Juvenile SBW marks were detected in the north-western corner of stratum 7S, and in strata 4, 5, and 7N at 300–380 m. These were 1 year-old fish (2015 year-class) with lengths between 12 and 19 cm. Juvenile marks also occurred outside the survey area in depths less than 300 m.

Biomass estimates were calculated for adult, immature, and juvenile SBW using the new target strength (TS) to fork-length (FL), length frequency information from commercial and research trawls, and the calculated sound absorption coefficient of 9.44 dB km^{-1}. The estimate of adult SBW biomass for all strata was 26 788 t (CV 35%) in the first snapshot and 113 274 t (CV 16%) in the second snapshot. Because the first snapshot did not cover the eastern aggregation, a combined adult estimate of 97 117 t (CV 16%) was obtained by averaging estimates for the northern and southern aggregations from the two snapshots, and using the snapshot 2 estimate for the eastern aggregation. The average estimate of immature SBW biomass for all strata was 4456 t (CV 19%), and the average estimate of juvenile biomass was 775 t (CV 37%). Adult SBW biomass in 2016 was 48% higher than the equivalent estimate from 2013, and the second highest in the time series, while immature SBW biomass was 44% lower than that in 2013, and below average for the time-series.

Tilt angle measurements were obtained for 262 individual SBW. These will be used to help address current uncertainty in acoustic target strength (TS) estimates for SBW.

1. INTRODUCTION

Southern blue whiting (*Micromesistius australis*) is one of New Zealand's largest volume fisheries, with annual landings of between 25 000 t and 40 000 t since 2000 (Ministry for Primary Industries 2016). Southern blue whiting (SBW) occur in Sub-Antarctic waters, with known spawning grounds on the Bounty Platform, Pukaki Rise, Auckland Islands Shelf, and Campbell Island Rise (Hanchet 1999). The SBW fishery was developed in the early 1970s by the Soviet fleet. Landings have fluctuated considerably, peaking at 76 000 t in the 1991–92 fishing year, when almost 60 000 t was taken from the Bounty Platform stock (Ministry for Primary Industries 2016). Southern blue whiting was introduced into the QMS from 1 April 2000 with separate TACs for each of the four main stocks in FMA 6. The Campbell Island stock (SBW 6I) is the largest of the four southern blue whiting stocks. The TACC for SBW 6I was increased to 39 200 t in 2014, but catches in the past two seasons have been below this level (Ministry for Primary Industries 2016).

Spawning occurs on the Bounty Platform from mid-August to early-September and three to four weeks later in the other areas. During spawning, SBW typically form large midwater aggregations. Commercial and research fishing on spawning SBW aggregations result in very clean catches of SBW. The occurrence of single-species spawning aggregations allows accurate biomass estimation using acoustics.

A time series of acoustic surveys for SBW on the Campbell Plateau was started in 1993. The acoustic surveys are used to measure relative abundance of adult SBW and also to predict pre-recruit numbers into the stock. The movement of fish during the survey period required the development of an adaptive survey design to increase efficiency. There were 11 previous surveys of the Campbell grounds: in 1993, 1994, 1995, 1998, 2000, 2002, 2004, 2006, 2009, 2011, and 2013). Biomass estimates of SBW in the three most recent surveys in 2009 (Gauthier et al. 2011), 2011 (O'Driscoll et al. 2012b), and 2013 (O'Driscoll et al. 2014) were relatively high, following the recruitment of the strong 2006 and 2009 year-classes into the fishery.

As SBW recruit at 2 and 3 years to the fishery, surveys are currently scheduled every 2–3 years to keep the assessment up to date. The acoustic survey of the Campbell Island stock scheduled for September 2015 was deferred to September 2016.

Knowledge of target strength (TS) is necessary for converting the backscatter attributable to SBW to an estimate of biomass. The relationship between TS and fork length (FL) for SBW was revised based on *in situ* TS data collected during the 2011 Campbell survey using an acoustic-optical system (O'Driscoll et al. 2013). This new relationship gives TS values within 1 dB of those estimated using the relationship recently adopted by ICES for blue whiting (*Micromesistius poutassou*) obtained from in situ measurements (Pedersen et al. 2011), but higher values than those estimated from the previous relationship for SBW, which was based on swimbladder modelling (Dunford & Macaulay 2006). O'Driscoll et al. (2013) found that the steep slope in the previous model estimates of SBW TS (Dunford & Macaulay 2006) was likely to be due to an inappropriate application of the Kirchhoff-approximation model at small swimbladder sizes, but noted that further work is required to attempt to reconcile differences between SBW swimbladder modelling and in situ TS results. During the 2016 survey, we proposed to try to further address the uncertainty in TS estimates by measuring the tilt angle distribution of SBW *in situ* using moored underwater video (O'Driscoll et al. 2012a).

1.1 Project objectives

This report summarises the data collected during the 12th research acoustic survey of SBW on the Campbell Island Rise in August–September 2016 and presents biomass estimates, fulfilling the reporting requirements for Objectives 1 and 2 of Ministry for Primary Industries Research Project DEE2016/02.

1. To estimate pre-recruit and spawning biomass at Campbell Island using an acoustic survey, with a target coefficient of variation (CV) of the estimate of 30%.

2. To collect *in situ* data on tilt-angle distribution and target strength of southern blue whiting and update the length to tilt-averaged target strength relationship as appropriate.

2. METHODS

2.1 Survey design

The time series of acoustic estimates for the Campbell Island SBW stock are from area-based surveys which provide fishery independent monitoring of the recruited part of the population as well as predicting the strength of year classes about to enter the fishery. An aggregation-based survey design is not appropriate for this fishery. Although much of the adult spawning biomass may be concentrated in one or more localised aggregations, a variable proportion of the biomass occurs away from these aggregations. The acoustic survey is also used to estimate abundance of pre-recruit SBW, which typically occur outside the area being fished by the commercial fleet. Attempts have been made to survey the main SBW spawning aggregations on the Campbell Island Rise from industry vessels in 2003 (O'Driscoll & Hanchet 2004), 2006 (O'Driscoll et al. 2006), and 2010 (O'Driscoll 2011), but these gave much lower estimates of SBW biomass than those obtained from wide-area surveys. For example, the aggregation-based survey by two industry vessels in 2006 gave estimates of abundance that were only 10–15% of those from the wide-area research survey in the same year (O'Driscoll et al. 2006, 2007).

The best time to survey SBW acoustically is when they aggregate to spawn. On the Campbell Island Rise the onset of spawning over the past 15 years has typically been from 6 to 17 September (range 3–20 September). The 2016 survey was carried out from 26 August to 23 September 2016 to maximise the chances of covering the spawning period. The 29-day booking of *Tangaroa* allowed for 21 days in the survey area, 1 day for acoustic calibration, 2 days for loading and unloading, and 5 days steaming to and from Wellington. Within the 21 days of survey time, allowance was made for 2 days for camera work (Objective 2), and 3 days for bad weather.

We aimed to carry out at least two snapshots of the Campbell Island Rise spawning area with an overall target CV of 30% (as specified by the project objectives). The survey followed the two-phase design recommended by Dunn & Hanchet (1998) and Dunn et al. (2001), incorporating the modifications recommended by Hanchet et al. (2003).

The initial stratification and transect allocation for snapshot 1 was based on that used in the most recent survey of the area in 2013 (O'Driscoll et al. 2014). Stratum boundaries were re-evaluated by examining the location of the commercial fishing fleet up to and including 2015 (Figure 1). The location of the commercial catch has varied considerably over time and in many years, including five of the six most recent years, a high proportion of the catch has been taken from outside the core survey area (strata 2–7). For 2016, we made two changes to the stratum boundaries used for snapshot 1 of the 2011 and 2013 surveys to reflect the more southerly distribution of SBW caught commercially in 2015 (Figure 1):

1. Stratum 8E was extended to the south (to 52° 40'S)
2. Stratum 7S was extended to the southwest (to 53° 35'S and 169° 24'E)

The proposed transect allocation for core strata in 2016 (Table 1) was similar to the allocation used for the last eight surveys.

During the first snapshot, the commercial fleet (only 4 vessels) was mainly fishing on the southern aggregation within stratum 7S (Figure 2). There was no evidence of fish in the southwest of stratum 7S,

where this stratum had been extended for snapshot 1. From about 10 September, vessels began fishing on the eastern aggregation in stratum 8S (Figure 2).

Several modifications were made to stratum boundaries for snapshot 2 based on the location of the main fish aggregations observed during snapshot 1 and the position of the fleet (Table 1, Figure 2). These were:

1. Reducing stratum 6S by shifting the southern boundary north from 53˚ 25'S to 52˚ 50'S.
2. Shifting the boundary between stratum 7N and stratum 7S north from 53˚ 12'S to 53˚ 06'S.
3. Reducing stratum 7S by shifting the southern boundary north from 53˚ 35'S to 53˚ 24'S and the western boundary east from 169˚ 24'E to 169˚ 50'E, along with the shift of northern boundary with stratum 7N from 53˚ 12'S to 53˚ 06'S.
4. Shifting the southern boundary of stratum 8S south from 52˚ 40'S to 52˚ 50'S.
5. Reducing the eastward extent of stratum 8E from 172˚ 10'E to 171˚ 45'E, and shifting the southern boundary south from 52˚ 40'S to 52˚ 50'S.

2.2 Acoustic data collection

NIWA's Simrad EK60-based towed system (Towbody 4), with a 38-kHz split-beam transducer, was used for most acoustic data collection along survey transects. A second Simrad EK60 towbody (Towbody 3) was carried as a spare, but was not required. Data were also collected using the hull-mounted EK60 system with 18, 38, 70, 120, and 200 kHz transducers throughout the voyage. The 38 kHz hull transducer was not transmitting during survey transects with the towed system to prevent interference, but was switched on when the towbody was onboard. The 38 kHz hull system was also used for some survey transects when the weather conditions were suitable.

The *Tangaroa* hull multifrequency echosounders and Towbody 4 were calibrated in East Bay, Marlborough Sounds at the start of the voyage on 27 August 2016. Both towed acoustic systems (Towbody 3 and 4) were also successfully calibrated in Perseverance Harbour at Campbell Island on 6–7 September, while sheltering from rough weather. Calibration reports are provided in appendices for the hull system (Appendix 1), Towbody 4 (Appendix 2), and Towbody 3 (Appendix 3).

Transect locations were randomly generated, and were carried out at right angles to the depth contours (i.e., from shallow to deep or vice versa). The minimum distance between transect midpoints varied between strata, and was calculated as follows:

$$m = 0.5 * L/n \quad (1)$$

where m is minimum distance, L is length of stratum, and n is the number of transects.

Transects were run at speeds of 6–10 knots (depending on the weather and sea conditions) with the acoustic towbody deployed 30–70 m below the surface. There is no evidence for a strong diel variation in SBW backscatter on the Campbell grounds (Hanchet et al. 2000a), so transects were carried out during day and night. Acoustic data collection was interrupted between transects for mark identification trawls.

2.3 Trawling

Trawling was carried out for mark identification, to collect biological data, and in support of tilt-angle data collection (see Section 2.4). Bottom marks were targeted using the 'ratcatcher' wing trawl, with 50 m sweeps, 50 m bridles, and a cod-end mesh of 40 mm. Midwater marks were targeted with the NIWA fine-mesh mesopelagic trawl with 10 mm codend Acoustic recordings were made for all trawls using the five frequency hull-mounted transducers.

Most target identification work was focused on:

1. establishing species mix proportions away from dominant heavy marks, which are easily identified as SBW;
2. distinguishing less dense adults marks from pre-recruit marks in areas where they occur in similar depths;
3. identifying the size and age composition of SBW in the less dense pre-recruit marks including 1, 2, and immature 3 year old fish;
4. obtaining a sample of adult SBW in areas which were not being fished by the commercial fleet.

Trawling was carried out both day and night. For each trawl all items in the catch were sorted into species and weighed on Marel motion-compensating electronic scales accurate to about 0.1 kg. Where possible, finfish, squid, and crustaceans were identified to species, and other benthic fauna to species or family. A random sample of up to 200 SBW and 50–200 of other important species from every tow was measured. In most tows the sex and macroscopic gonad stage (Appendix 4) of all SBW in the length sample were also determined. More detailed biological data were collected on a subsample of up to 20 SBW per trawl, and included fish length, weight, sex, gonad stage, gonad weight, and occasional observations on stomach fullness and contents, and prey condition. Otoliths were also collected from up to 20 SBW per trawl to augment those collected by the scientific observer programme.

Estimated SBW length frequencies from research trawls were constructed by scaling length frequencies from individual tows by the SBW catch in the tow.

2.4 Underwater camera deployments

To try to address current uncertainty in acoustic target strength (TS) estimates for SBW (O'Driscoll et al. 2013), we attempted to measure the tilt angle distribution of SBW *in situ* using underwater video. We proposed using moored video equipment, comprising a string of up to three GoPro digital handy-cams mounted inside custom-built pressure housings with associated lights, batteries, and a microprocessor controller (described in detail by O'Driscoll et al. 2012a). The microprocessor allowed the camera and lights to be set to go on and off periodically. O'Driscoll et al. (2012a) have suggested that the first video frame after the lights come on may provide the best estimate of tilt angles of undisturbed fish *in situ*.

The use of moorings requires approval from the Environmental Protection Agency (EPA) under the Exclusive Economic Zone and Continental Shelf (Environmental Effects–Permitted Activities) Regulations 2013. This EPA permit number was NIWAPA15.

2.5 Other data collection

A Seabird SM-37 Microcat CTD datalogger (serial number 2958) was mounted on the headline of the net during 19 bottom trawls to determine the absorption coefficient and speed of sound, and to define water mass characteristics in the area (Appendix 5). CTD drops were also carried out in conjunction with the three acoustic calibrations.

2.6 Commercial catch data

Additional information on the species composition, size, and spawning state of adult SBW in the survey area was obtained from commercial catch data collected by scientific observers. Data from the 2016 fishery were extracted from the Ministry for Primary Industries cod database on 20 November 2016. Scaled length frequency distributions were calculated as the weighted (by catch) average of individual length samples. Data on female gonad stage (using the five-stage observer scale) were summarised by date.

2.7 Acoustic data analysis

Acoustic data collected during the survey were analysed using standard echo-integration methods (Simmonds & MacLennan 2005), as implemented in NIWA's Echoanalysis (ESP3) software.

Echograms were visually examined, and the bottom determined by a combination of an in-built bottom tracking algorithm and manual editing. Regions were then defined corresponding to different acoustic mark types. Following the approach used in previous years, SBW acoustic marks were initially classified into adult (recruited fish), immature (mainly 2 year olds), and juvenile (1 year olds). Marks were classified subjectively, based on their appearance on the echogram (shape, structure, depth, strength, etc.), and using information from research trawls. Hanchet et al. (2002) provided representative examples of the different mark types.

Backscatter from regions identified as SBW was then integrated to produce an estimate of acoustic density (m^{-2}). During integration acoustic backscatter was corrected for the sound absorption by seawater. The calculated sound absorption for the area based on CTD data was 9.44 dB km^{-1} (Appendix 5).

Acoustic density was output in two ways. First, average acoustic density over each transect was calculated. These values were used in biomass estimation (see Section 2.8). Second, acoustic backscatter was integrated over 10-ping bins (vertical slices) to produce a series of acoustic densities for each transect (typically 100–700 values per transect). These data had a high spatial resolution, with each value (10 pings) corresponding to about 100 m along a transect, and were used to produce plots showing the spatial distribution of acoustic density (see Section 3.4).

2.8 Biomass estimation

Acoustic density estimates were converted to SBW biomass using the ratio, *r*, of mean weight to mean backscattering cross-section (linear equivalent of target strength). Acoustic target strength was derived using the new target-strength-to-fork-length (TS-FL) relationship of O'Driscoll et al. (2013):

$$TS = 22.06 \log_{10} FL - 68.54 \quad (2)$$

Where TS is in decibels (dB re $1m^2$) and FL in centimetres (cm).

SBW weight, w (in grams), was determined using the combined length-weight relationship for spawning SBW from Hanchet (1991):

$$w = 0.00439 * FL^{3.133} \quad (3)$$

Mean weight and mean backscattering cross-section (linear equivalent of TS) for each category (adult by area, immature, and juvenile) were obtained by transforming the scaled length frequency distribution for both sexes combined by Equations 3 and 2 respectively, and then calculating the means of the transformed distributions.

Biomass estimates and variances were calculated from transect density estimates using the formulae of Jolly & Hampton (1990). The mean SBW stratum density for each category was multiplied by the stratum area to obtain biomass estimates for each stratum, which were then summed over all strata to produce an estimate for the snapshot. The two snapshots were averaged to produce the survey estimate. The sampling precision (CV) of the mean biomass estimate from the survey combined the variance from each snapshot, assuming that each snapshot was independent.

No towbody motion correction (Dunford 2005) was applied to biomass estimates, as measurements of towbody pitch and roll are not available for all surveys in the time-series. O'Driscoll et al. (2007) indicated that compensating for motion correction increased biomass by only 3–10% in 2006. As expected, the magnitude of the change due to motion correction was related to mark depth (larger effect with increasing depth) and sea conditions (larger effect in poor conditions when there was greater towbody motion).

Acoustic biomass estimates are no longer decomposed to provide estimates of 1, 2, 3, and age 4+ fish (Hanchet et al. 2000b), as this is now done within the assessment model.

2.9 Tilt angle estimation

The software Sony Vegas Pro12 was used to view the video and generate screen grabs. Quantitative analysis was based on still images (frame grabs) selected from the recording. The first selected image was the frame when the lights first went on, which we regarded as the best measure of undisturbed fish density and orientation. Image analysis was carried out using Image–J software. Measurements of fish fork length (in pixels) and orientation were made for SBW that appeared to be side-on to the camera.

3. RESULTS

3.1 Data collection

All survey objectives were achieved despite the loss of about 117 h (5 days) of survey time due to poor weather conditions. This exceeded the weather allowance of three days provided for in the survey design. Rough weather was encountered while steaming south at the beginning of the survey and our arrival in the survey area was delayed by 24 hours. Strong winds and large swells stopped work, and we were forced to seek shelter at Campbell Island, for 48 hours on 6–7 September and 45 hours on 13–15 September. Although weather and sea conditions allowed collection of acoustic data for the rest of the voyage, they were often marginal, with 25–40 knot winds (Figure 3) and 4–8 m swells. These conditions reinforced the value of using specialist towed acoustic systems, as data quality on the hull echosounders was poor. Good weather during the last week of the voyage (16–20 September) allowed us to carry out experimental camera work for Specific Objective 2 and complete all planned transects in snapshot 2. A total of 57.2 GB of acoustic data made up of 509 files (145 Towbody 4 and 364 hull) were recorded during the survey.

Nineteen bottom trawls and one midwater trawl were carried out to identify targets and collect biological samples (Table 2, Figures 4–5). Tow length ranged from 0.02 to 1.73 n. miles at an average speed of 3.4 knots (Table 2). The total trawl catch was 5903 kg. This was made up of 56 species or species groups (Table 3). Most tows were dominated by southern blue whiting (55.5% of total catch, see Table 2). The most abundant bycatch species were floppy tubular sponges (12.1%, mainly from one trawl), ling (8.5%), oblique banded rattail (5.5%), javelinfish (5.4%), and pale ghost shark (3.8%). A random sample of all quota, commercially important, and selected non-commercial species were measured from all stations. A total of 8036 fish and squid of 33 different species were measured (Table 3). Otoliths were collected from 363 SBW for ageing.

Due to poor weather conditions, no moorings were attempted in the first three weeks of the voyage. Instead the mooring cameras were lowered from the vessel into a SBW aggregation in stratum 7S on 9–10 September, and an aggregation in stratum 8S on 12 September. Camera and lights were timed to go on for 30 minutes every hour, and behaviour of the aggregation was monitored using the hull-mounted echosounders. Three camera deployments were made in this manner (stations 8, 9, 14 in Table 2). In the first (station 8) and third (station 14) deployments, only a single camera was used. In the second camera deployment (station 9), two cameras were lowered, but the lights only worked on the lower camera. With improved weather conditions in the last week of the voyage, we were able to deploy our moored cameras overnight on 17–18 September. The mooring was deployed in a large aggregation

in stratum 4 (station 19 in Table 2) at 15:41 NZST on 17 September and recovered at 10:47 on 18 September. Cameras were positioned 10 m and 90 m above the seabed and were set to record for 2 minutes every hour. During the mooring deployment the aggregation was monitored using the hull-mounted echosounders. On the final night in the survey area (19–20 September) we carried out a further camera drop where two mooring cameras were lowered from the vessel into a SBW aggregation in stratum 4 (station 24 in Table 2). The cameras and lights were 20 m apart and were timed to go on for 2 minutes every 30 minutes. The vessel drifted for 13 hours and the aggregation was 'followed' by changing the wire length to match the depth of highest density observed on the hull-mounted echosounders.

The 19 CTD profiles showed that the water column was unstratified with surface temperatures ranging between 7.2 and 7.5 °C (see Appendix 5).

3.2 Commercial data

A total of 409 target SBW tows were reported on trawl catch effort processing return (TCEPR) forms from the Campbell Island grounds between 24 August and 3 October 2016, for a total estimated catch of 15 112 t of SBW. This was slightly lower than the reported (QMR) catch of 18 635 t for SBW 6I and much less than the TACC of 39 200 t. The catch rates from commercial trawls during the 2016 season are shown in Figure 6. Fishing effort was concentrated in the eastern and southern areas throughout the season, with only 22 tows (252 t of SBW catch) in the north. As in 2013, the fishing pattern in 2016 was strongly influenced by bycatch of sea-lions, and associated reluctance to fish away from the fleet (Richard Wells, Deepwater Group Ltd, pers. comm.). During the first snapshot, fishing effort was concentrated in stratum 7S, but effort was more widespread in strata 6S, 7N, 7S, 8S, and 8E during snapshot 2 (see Figure 2).

Two distinct spawning periods (defined as when the proportion of running ripe females exceeded 10%) were recorded, from 1–8 September and from 17–25 September (Figure 7). The timing of the first spawning in 2016 was similar to that in 2013, and relatively early compared to the timing in previous survey years (Figure 7).

The scaled length frequency distributions of SBW caught by commercial vessels are shown in Figure 8. Length distributions were unimodal for males centred on about 35 cm, and bimodal for females with modes centred on about 37 cm and 45 cm (Figure 8). Although there were very few trawls sampled in the northern area (SBW only measured from 4 commercial tows), there appeared to be a lower proportion of fish larger than 40 cm in the north, compared to the east and south, and the mean length was lower in the north (Table 4). The length frequency distributions from the eastern and southern areas were similar (Figure 8, Table 4), but the proportion of males was higher in the measured catch in the east (62% male) than in the south (53% male).

3.3 Mark identification

Mark types were generally similar to those described for SBW on the Campbell Island Rise by Hanchet et al. (2002). As in previous years, most of the main adult marks were relatively easy to identify by their appearance and location in the water column.

Pre-spawning adult SBW marks were detected during snapshot 1 in strata 2 and 4 on 31 August to 2 September, at about 430–480 m bottom depth). These were typically about 20 m off the bottom during the day and extending 60–100 m off the bottom at night (Figure 9). No strong marks were detected in the east, but a small pre-spawning aggregation was observed in stratum 8S on 5 September (Figure 9). The densest concentration during snapshot 1 was in stratum 7S on 9 September, and was up to 100 m in height at night (Figure 9).

A large aggregation was found in the eastern area (centred in stratum 8S, but extending into strata 6S and 8E) during snapshot 2 on 11–13 September (Figure 10). Gonad stage information (Table 5) suggested that these eastern fish had already spawned once before 11 September, but would be likely to spawn a second time. Dense aggregations were also observed in strata 2, 4, and 5 on 16–19 September (Figure 10), east of where the northern aggregation was detected in snapshot 1. Most of the northern fish we caught were post-spawning (i.e., spent), although some fish were still actively spawning (i.e., running ripe) on 17–18 September (Table 5).

Immature southern blue whiting marks (Figure 11) were widespread at depths from 370–410 m. These were fish with lengths between 25 and 30 cm (see Figure 8) and were probably 2 or 3 years old (2014 or 2013 year-class). Juvenile SBW marks were sometimes detected at 300–380 m (Figure 11). These were 1 year-old fish (2015 year-class) with lengths between 12 and 19 cm (see Figure 8).

Weak background demersal marks (bottom "fuzz") was widespread throughout the survey area, but trawls indicated that these contained a low proportion of SBW (see Table 2). Mesopelagic fish marks were also common, particularly in the south. During the day mesopelagic marks were observed as a series of schools between 50 and 300 m depth. These schools tended to disperse at night.

No species decomposition of acoustic backscatter was attempted because of the small number of trawls and uncertainty associated with the relative catchabilities of different species. All backscatter from adult, juvenile, and immature marks was assumed to be from SBW, which was consistent with mark identification in previous years and supported by the majority of previous trawl catches (Hanchet et al. 2003, O'Driscoll et al. 2007, 2012b, Gauthier et al. 2011). The acoustic contribution of SBW in the background demersal fuzz marks was ignored.

3.4 Distribution of SBW backscatter

Expanding symbol plots show the spatial distribution of adult, immature, and juvenile SBW along each transect during the two acoustic snapshots (Figures 12–14). As noted in Section 3.3, adults were detected mainly in the north (strata 2 and 4) and south (stratum 7S) during snapshot 1. No strong marks were detected in the east in snapshot 1, with only a small pre-spawning aggregation in stratum 8S (Figure 12). Much more extensive adult marks were detected in the eastern area (strata 6N, 6S, 8S, and 8E) during snapshot 2 (Figure 12). The southern aggregation was in a similar position in snapshots 1 and 2, as both snapshots of this area occurred over a short time period on 8–11 September. The northern aggregation was more dispersed in snapshot 2 and was spread through strata 2, 4, and 5 (Figure 12)

Immature SBW marks occurred in depths shallower than 410 m in strata 2, 4, 5, 7N, and 7S (Figure 13) and juveniles were detected in the north-western corner of stratum 7S, and in strata 4, 5, and 7N at 300–380 m (Figure 14). Consistent with previous surveys, the western (shallow) survey boundary was at 300 m depth. Juvenile marks were observed while steaming shallower than 300 m, but the survey priority was to estimate abundance of adult SBW so there was insufficient time to fully explore the likely distribution of juvenile SBW.

3.5 SBW size and maturity

Length, sex, and gonad stage were determined for 3765 SBW during the survey (see Table 3). The scaled length frequency distributions from research tows on adult, immature, and juvenile marks are compared to data from the commercial fishery in Figure 8. The size distributions of fish from research tows on adult aggregations in the north and east were generally similar to those from the commercial catch (see Figure 8, Table 4). As in the commercial data, adult fish from the eastern aggregation were larger on average (mean length of all SBW, 38.1 cm) than those from the north (mean length, 35.3 cm). Fish caught from immature

marks had a single mode between 25 and 30 cm, and were probably 2 or 3 years old (2014 or 2013 year-class). Juveniles were 12–19 cm (2015 year-class).

Inferences about timing of spawning cannot be made from research data because of the small number of tows and also because much of the fishing was outside the main spawning aggregations. Almost all adult female SBW caught in snapshot 1 were pre-spawning (stage 3), and most adult females caught in snapshot 2 were post-spawning (stages 6–7) (Table 5, see Appendix 4 for description of research stages). Running ripe female SBW (stage 5) were observed in research trawls in stratum 4 on 17–18 September, and occasionally at other times (Table 5). Both males and females in the immature category were almost exclusively stage 1.

3.6 SBW biomass estimates

The values of *r* for each SBW category based on the length frequency distributions in Figure 8 are given in Table 4. The ratios for juvenile SBW, immature SBW, and adult SBW in the northern area (where there was little commercial effort) were calculated from the scaled length frequency distribution of SBW from research trawls by *Tangaroa* during the survey. The ratios for adult SBW in the southern and eastern areas was calculated using the scaled length frequency distribution of the commercial catch from observer data.

SBW biomass estimates by snapshot and stratum are given in Table 6. These estimates were calculated using the TS-length relationship of O'Driscoll et al. (2013) and a calculated sound absorption coefficient of 9.44 dB km^{-1} (see Appendix 5). Note that the estimates in Table 6 are not directly comparable with those from previous SBW acoustic survey reports which used older estimates of sound absorption (typically 8.0 dB km^{-1}) and TS (Fu et al. 2013).

The adult biomass estimate was 26 788 t (CV 35%) in snapshot 1 and 113 274 t (CV 16%) in snapshot 2. The four-fold difference between snapshot estimates was driven by an order of magnitude increase in the estimated biomass in the eastern area from 4368 t in snapshot 1 to 58 540 t in snapshot 2, and a trebling of the biomass in the northern area from 15 560 t in snapshot 1 to 45 751 t in snapshot 2 (Figure 15). Estimates from the two snapshots of the southern area were relatively similar, at 6861 t in snapshot 1 and 8983 t in snapshot 2 (Figure 15). Most (84%) of the adult biomass in the first snapshot was within the historical core area (strata 2–7), but only 51% was in the core area in snapshot 2. Variability between snapshots and derivation of the acoustic abundance index for 2016 is discussed in Section 4.2.

The estimate of immature SBW biomass for all strata was 6252 t (CV 23%) in the first snapshot and 2660 t (CV 36%) in the second snapshot, giving an average immature estimate of 4456 t (CV 19%) (Table 6). Estimated juvenile biomass was 624 t (CV 68%) in the first snapshot and 926 t (CV 42%) in the second snapshot, giving an average juvenile estimate of 775 t (CV 37%).

3.7 Tilt angle estimates

Southern blue whiting reacted by diving as the camera frame (without the lights on) was lowered into the aggregation, but re-formed around the camera (e.g. Figure 16). When the lights were turned on, the fish scattered (e.g., Figures 16–17).

The five camera deployments provided 262 measurements of tilt angles from SBW, most (85%) of which came from the two lowered cameras at station 24 (see Figure 17). The tilt angle distribution changed in response to the lights, with a broader distribution of tilt angles 30–100 seconds after the lights came on (Figure 18). Only 10 SBW were measured in the first camera frame after the lights came on, which we interpret as being the most representative of undisturbed fish. These 10 fish had a mean tilt angle of -2.5° with standard deviation 14.2° (Figure 18). Although sample sizes were small, this tilt

angle distribution was quite similar to estimated swimming angles from AOS (mean 16°, standard deviation 15° from O'Driscoll et al. 2013). The 2016 survey showed that the methodology worked for SBW, and we recommend further *in situ* measurements be made using lowered cameras on future voyages to increase the sample size. Tilt angle distributions can then be developed to help improve estimates of SBW TS. Because of the small sample size from 2016 we did not run the observed tilt angle distribution through the TS swimbladder model.

4. DISCUSSION

4.1 Timing of the survey

The timing and duration of the 2016 survey were similar to those in the previous six surveys (2002, 2004, 2006, 2009, 2011, and 2013). The survey was about one week earlier than those before 2002 (see Figure 7). In 2016, the first spawning occurred relatively early, from about 1–8 September, with a second peak from 17–25 September (see Figure 7). The timing of the survey relative to spawning was appropriate, with snapshot 1 (31 August – 10 September) surveying pre-spawning and spawning fish, and snapshot 2 (10–20 September) surveying post-spawning and spawning fish.

4.2 Variability between snapshots

The four-fold difference in adult SBW biomass estimates between snapshots 1 and 2 in 2016 was greater than that observed in any of the other surveys in the Campbell time-series, with the maximum difference observed previously between snapshots only a factor of 2.5 (in 2002) (Figure 19). The 2016 survey was also the first survey where the two snapshot estimates did not have overlapping 95% confidence intervals (Figure 19). As noted in Section 3.6, the difference between snapshot estimates was driven by an order of magnitude increase in the estimated biomass in the eastern area from snapshot 1 to snapshot 2, and a trebling of the biomass in the northern area. Despite more extensive coverage of the eastern area than in any previous acoustic survey, only weak adult marks were detected in the east in snapshot 1 (see Figure 12). A week later, in snapshot 2, there were extensive post-spawning marks, centred in stratum 8S, but extending into strata 6N, 6S and 8E (Figure 12). These marks were found within the area that was covered during snapshot 1, but were also observed further south, and the southern boundaries of strata 8S and 8E were shifted 10 n. miles south from 52˚ 40'S to 52˚ 50'S for snapshot 2 (see Figure 2). Even with this southward extension, adult SBW were detected on the southernmost transects in strata 8S and 8E. However there was no commercial fishing effort south of the snapshot 2 boundary (see Figure 2), which suggests that the surveyed area was appropriate and encompassed most of the fish.

There are at least two potential hypotheses to explain the low estimated biomass of adult SBW in the eastern area during snapshot 1:

1. Fish were outside the surveyed area;
2. Fish were inside the surveyed area, but were densely aggregated and were between transects.

There is little information available to discriminate between these hypotheses. There was almost no commercial fishing effort within the eastern area in snapshot 1, and the few tows that did occur were within the survey boundaries (see Figure 2). As noted above, the spatial coverage in snapshot 1 was greater than in any previous Campbell acoustic survey, and encompassed all commercial effort in recent years (see Figure 1). As far as we are aware, there has never been any fishing for spawning SBW east of 171˚ E and south of 52˚ 40' S. If spawning SBW occurred outside the snapshot 1 survey area, this represents an extension of the eastern spawning area (see Section 4.3).

Transects in the eastern area during snapshot 1 on 3–6 September were carried out when fish were actively spawning in the south (see Figure 7). During spawning, SBW sometimes form very dense

schools (Hanchet et al. 2002). The transect spacing in stratum 8E during snapshot 1 averaged 16 km, with the maximum gap between adjacent random transects of 25 km. It is possible that an eastern spawning aggregation was present within the survey area but was not intersected by any of the transects. This almost occurred on the previous survey in 2013, when adult SBW were detected between, and slightly east of, transects in stratum 8E while steaming, and a small additional stratum was added to encompass the full extent of this aggregation (O'Driscoll et al. 2014). This additional stratum (stratum 10) accounted for 43% of the adult biomass observed in snapshot 1 of the 2013 survey (O'Driscoll et al. 2014).

Regardless of the reason for the low eastern biomass estimate in snapshot 1, it is not statistically appropriate to average abundance estimates from this region from the two snapshots, as 95% confidence intervals do not overlap (see Figure 15). At its meeting on 5 December 2016, the Deepwater Fisheries Assessment Working Group agreed that the 'best' estimate of adult SBW biomass in 2016 was calculated by averaging the two snapshot estimates for the northern and southern aggregations, and adding the snapshot 2 estimate for the eastern aggregation. This gave an estimate of 97 117 t (CV 16%) (Table 7).

The estimates of immature and juvenile SBW in 2016 were relatively consistent between snapshots (see Table 6), although the spatial distribution differed (see Figures 13–14). The Deepwater Fisheries Assessment Working Group agreed that the average estimate of the two snapshots provided the 'best' 2016 estimates for immature and juvenile SBW (Table 7).

4.3 Treatment of fish outside the core survey area

Historically, the Campbell SBW fishery was characterised as occurring on two distinct aggregations: northeastern, and southern (e.g., 2010 in Figure 1), which often had different fish length structure (Hanchet 1998, 2005). The location of the northeastern aggregation has varied, and, since 2002, there has been increasing commercial catch and effort outside the historical core survey area (see Figure 1). Hanchet (2005) examined commercial length frequency data from 1997 to 2004 and found that SBW caught east of the core area had a similar size distribution to those caught in the north within the core area, so concluded that changes in fish distribution were likely to be due to fish movement rather than appearance of previously unsurveyed fish. In 2011 and 2013, the single aggregation in the northeast split into two distinct aggregations in the north and east (O'Driscoll et al. 2012b, 2014), and commercial data also supported the existence of separate aggregations in the north and east in 2011, 2012, and 2015 (see Figure 1).

At the same time as the distribution of SBW expanded in the north and east, the relative contribution of the southern aggregation declined. In 2009, very dense spawning marks were detected in the south and the southern aggregation accounted for 24% of the estimated adult acoustic biomass on the Campbell Island Rise (Gauthier et al. 2011). This had declined to only 3% of the estimated adult biomass in 2011 (O'Driscoll et al. 2012b), and, despite extensive searching, no spawning SBW were detected in the south in 2013 (O'Driscoll et al. 2014). Commercial catch rates in the south also declined, with only 5 trawls in this area in 2013, but the aggregation reappeared in 2014 and 2015 (see Figure 1).

In 2016, the acoustic survey observed three adult aggregations, in the north, east, and south. Most commercial fishing effort was in the east and south (see Figure 6), but dense acoustic marks were observed in the northern area in both snapshots (see Figures 9 and 10). All fish recorded during the 2016 survey were used for the biomass estimates. The estimated relative contribution of the three regions to the 'best' adult acoustic abundance estimate in 2016 was: north, 32%; east, 60%, and south, 8%.

The eastern and southern aggregations had similar length distributions (see Figure 8). It appears that the southern aggregation moved northeast during the survey, while the eastern aggregation moved

southwest (see Figure 2), so it is possible that fish caught in stratum 7N, which were counted as 'southern fish' may have been a mixture of fish from the east and south. Research trawls caught smaller SBW on average in the north than from tows in the east (see Figure 8). There were only 4 commercial tows observed in the northern area, but these also had a lower proportion of SBW greater than 40 cm than tows in the east and south (see Figure 8). The northern aggregation appeared to move southeast during the survey period (see Figure 12).

In light of continuing changes in the distribution of SBW, we recommend that the survey area and stratification continues to be reviewed before future surveys.

4.4 Comparison between years

The acoustic biomass estimate for adult SBW increased by 48% from the previous survey in 2013 (see Table 7), which is consistent with relatively good recent recruitment and recent catches well below the TACC (Ministry for Primary Industries 2016). Both the 2006 and 2009 year-classes have been estimated as being relatively strong (Dunn & Hanchet 2015) and SBW from these year-classes probably account for many of the larger fish caught in 2016 (see Figure 8). O'Driscoll et al. (2014) reported that biomass of immature SBW in 2013 was about average for the time-series, suggesting average recruitment of the 2011 year-class. These were fish of age 5 in 2016, and account for the mode of fish at around 35 cm in 2016 (see Figure 8).

The estimated abundance of immature SBW in 2016 was 44% lower than that in 2013, and below average for the time-series (see Table 7). This suggests that 2013 (3 year old) and 2014 (2 year old) year-classes were not particularly strong. Although not well indexed by the survey (because they also occur shallower than 300 m), the observation of some juvenile SBW indicates the presence of the 2015 year-class at age 1.

5. ACKNOWLEDGMENTS

Thanks to the officers and crew of the *Tangaroa* and to the scientific staff for making this a successful voyage despite adverse weather conditions. Special thanks to Pablo Escobar-Flores who was a late replacement. New Zealand Diving Services and Bruce Lines provided dive support for the acoustic calibration in the Marlborough Sounds. We are also grateful to skippers, fishing masters, and company representatives on other vessels fishing on the Campbell grounds for providing and sharing information. Once again, weather forecasts were provided to the ship from Ecoconnect by Bernard Miville and David Sullivan and these were helpful in making operational decisions. This research was funded by Ministry for Primary Industries project DEE2016/02. Ian Doonan reviewed a draft of this report and made a number of helpful comments.

6. REFERENCES

Demer, D.A.; Berger, L.; Bernasconi, M.; Bethke, E.; Boswell, K.; Chu, D.; Domokos, R., et al. (2015). Calibration of acoustic instruments. *ICES Cooperative Research Report No. 326*. 133 p.

Doonan, I.J.; Coombs, R.F.; McClatchie, S. (2003). The absorption of sound in seawater in relation to the estimation of deep-water fish biomass. *ICES Journal of Marine Science 60*: 1047–1055.

Dunford, A. (2005). Correcting echo integration data for transducer motion. *Journal of the Acoustical Society of America 118*: 2121–2123.

Dunford, A.J.; Macaulay, G.J. (2006). Progress in determining southern blue whiting (*Micromesistius australis*) target strength: results of swimbladder modelling. *ICES Journal of Marine Science 63:* 952–955.

Dunn, A.; Grimes, P.J.; Hanchet, S.M. (2001). Comparative evaluation of two-phase and adaptive cluster sampling designs for acoustic surveys of southern blue whiting (*M. australis*) on the Campbell Rise. Final Research Report for Ministry of Fisheries Research Project SBW1999/01. Objective 1. 15 p. (Unpublished report held by Fisheries New Zealand, Wellington.)

Dunn, A.; Hanchet, S.M. (1998). Two-phase acoustic survey designs for southern blue whiting on the Bounty Platform and the Pukaki Rise. *NIWA Technical Report 28.* 29 p.

Dunn, A.; Hanchet, S.M. (2015). Review and summary of the time series of input data available for the assessment of southern blue whiting (*Micromesistius australis*) stocks up to and including the 2013 season. *New Zealand Fisheries Assessment Report 2015/56*. 45 p.

Fofonoff, P.; Millard, R., Jr (1983). Algorithms for computation of fundamental properties of seawater. *UNESCO Technical Papers in Marine Science 44*. 53 p.

Francois, R.E.; Garrison, G.R. (1982). Sound absorption based on ocean measurements. Part II: Boric acid contribution and equation for total absorption. *Journal of the Acoustical Society of America 72*: 1879–1890.

Fu, D.; Hanchet, S.; O'Driscoll, R.L. (2013). Estimates of biomass and c.v.s of southern blue whiting from previous acoustic surveys from 1993 to 2012 using a new target strength – fish length relationship. Final Research Report for Ministry for Primary Industries Research Project DEE201002SBWB. 52 p. (Unpublished report held by Fisheries New Zealand, Wellington.)

Gauthier, S.; Fu, D.; O'Driscoll, R.L.; Dunford, A. (2011). Acoustic estimates of southern blue whiting from the Campbell Island Rise, August–September 2009. *New Zealand Fisheries Assessment Report 2011/9*. 40 p.

Hanchet, S.M. (1991). Southern blue whiting fishery assessment for the 1991–92 fishing year. New Zealand Fisheries Assessment Research Document 91/7. 48 p. (Unpublished report held in NIWA library, Wellington.)

Hanchet, S.M. (1998). A review of southern blue whiting (*Micromesistius australis*) stock structure. New Zealand Fisheries Assessment Research Document 98/8. 28 p. (Unpublished report held in NIWA library, Wellington.)

Hanchet, S.M. (1999). Stock structure of southern blue whiting (*Micromesistius australis*) in New Zealand waters. *New Zealand Journal of Marine and Freshwater Research 33*: 599–610.

Hanchet, S.M. (2005). Southern blue whiting (*Micromesistius australis*) stock assessment update for the Campbell Island Rise for 2005. *New Zealand Fisheries Assessment Report 2005/40*. 40 p.

Hanchet, S.M.; Bull, B.; Bryan, C. (2000a). Diel variation in fish density estimates during acoustic surveys of southern blue whiting. *New Zealand Fisheries Assessment Report 2000/16*. 22 p.

Hanchet, S.M.; Grimes, P.J.; Coombs, R.F.; Dunford, A. (2003). Acoustic biomass estimates of southern blue whiting (*Micromesistius australis*) for the Campbell Island Rise, August-September 2002. *New Zealand Fisheries Assessment Report 2003/44.* 38 p.

Hanchet, S.M., Grimes, P.J.; Dunford, A.; Ricnik, A. (2002). Classification of fish marks from southern blue whiting acoustic surveys. Final Research Report for Ministry of Fisheries Research Project SBW2000/02 Objective 2. 55 p. (Unpublished report held by Fisheries New Zealand, Wellington.)

Hanchet, S.M.; Richards, L.; Bradford, E. (2000b). Decomposition of acoustic biomass estimates of southern blue whiting (*Micromesistius australis*) using length and age frequency data. *New Zealand Fisheries Assessment Report 2000/43.* 37 p.

Jolly, G.M.; Hampton, I. (1990). A stratified random transect design for acoustic surveys of fish stocks. *Canadian Journal of Fisheries and Aquatic Sciences 47*: 1282–1291.

MacLennan, D.N. (1981). The theory of solid spheres as sonar calibration targets. *Scottish Fisheries Research 22*. 17 p.

Ministry for Primary Industries (2016). Fisheries Assessment Plenary, May 2016: stock assessments and stock status. Compiled by the Fisheries Science Group, Ministry for Primary Industries, Wellington, New Zealand. 1556 p.

O'Driscoll, R.L. (2011). Acoustic biomass estimates of southern blue whiting on the Pukaki Rise and Campbell Island Rise in 2010. NIWA Client Report WLG2011-03 for The Deepwater Group Ltd. 37 p. (Unpublished report available from Deepwater Group Ltd, Nelson.)

O'Driscoll, R.L.; de Joux, P.; Nelson, R.; Macaulay, G.J.; Dunford, A.J.; Marriott, P.M.; Stewart, C.; Miller, B.S. (2012a). Species identification in seamount fish aggregations using moored underwater video. *ICES Journal of Marine Science 69*: 648–659.

O'Driscoll, R.L.; Dunford, A.J.; Fu, D. (2012b). Acoustic estimates of southern blue whiting from the Campbell Island Rise, August–September 2011 (TAN1112). *New Zealand Fisheries Assessment Report 2012/18*. 52 p.

O'Driscoll, R.L.; Dunford, A.J.; Ladroit, Y. (2014). Acoustic estimates of southern blue whiting from the Campbell Island Rise, August–September 2013 (TAN1309). *New Zealand Fisheries Assessment Report 2014/22*. 46 p.

O'Driscoll, R.L.; Hanchet, S.M. (2004). Acoustic survey of spawning southern blue whiting on the Campbell Island Rise from FV *Aoraki* in September 2003. *New Zealand Fisheries Assessment Report 2004/27*. 31 p.

O'Driscoll, R.L.; Hanchet, S.M.; Gauthier, S.; Grimes, P.J. (2007). Acoustic estimates of southern blue whiting from the Campbell Island Rise, August-September 2006. *New Zealand Fisheries Assessment Report 2007/20.* 34 p.

O'Driscoll; R.L.; Macaulay, G.J.; Gauthier, S. (2006). Biomass estimation of spawning southern blue whiting from industry vessels in 2006. NIWA Client Report: WLG2006-89 for the Deepwater Stakeholders Group Ltd. 43 p. (Unpublished report available from Deepwater Group Ltd, Nelson.)

O'Driscoll, R. L.; Oeffner, J.; Dunford, A.J. (2013). *In situ* target strength estimates of optically verified southern blue whiting (*Micromesistius australis*). *ICES Journal of Marine Science 70*: 431–439.

Pedersen, G.; Godø, O.R.; Ona, E.; Macaulay, G.J. (2011). A revised target strength–length estimate for blue whiting (*Micromesistius poutassou*): implications for biomass estimates. *ICES Journal of Marine Science 68*: 2222–2228.

Simmonds, E.J.; MacLennan, D.N. (2005). Fisheries acoustics. Second edition. Blackwell Science, Oxford. 437 p.

7. TABLES

Table 1: Summary of transects carried out during the 2016 SBW acoustic survey of the Campbell Island Rise. Transect positions are plotted in Figures 4–5. Snapshot 1 transect allocation proposed for the 2016 acoustic survey of the Campbell Island Rise, based on historical mean fish densities and commercial tow positions. Strata 2–7 are core strata which have been surveyed in all previous acoustic surveys. Note that the boundaries of strata 6S, 7N, 7S, 8S, and 8E were modified for Snapshot 2 (areas in bold).

	Snapshot 1 (31 Aug – 10 Sep)		Snapshot 2 (10–20 Sep)	
Stratum	Area (km^2)	Number of transects	Area (km^2)	Number of transects
2	3 154	5	3 154	5
3N	2 342	3	2 342	3
3S	1 013	3	1 013	3
4	2 690	5	2 690	5
5	3 029	4	3 029	4
6N	1 150	4	1 150	3
6S	3 025	3	**1 577**	5
7N	2 980	4	**2 322**	3
7S	3 815	8	**2 035**	6
8N	1 436	3	1 436	3
8S	1 452	3	**1 978**	5
8E	4 648	6	**2 070**	8
Total	30 734	51	24 796	53

Table 2: Station details and catch of southern blue whiting (SBW) during the 2016 acoustic survey of the Campbell Island Rise. Station positions are plotted in Figures 4 and 5. Mark type: Adult, adult SBW; Imm, immature SBW; Juv, juvenile SBW; Back, background fuzz; Meso, mesopelagic. Gear type: BT, bottom trawl; Camera, drop camera; MW, midwater trawl; Mooring, moored camera.

Tow	Date	Mark type	Gear type	Stratum	Latitude (° 'S)	Longitude (° 'E)	Tow depth (m)	Distance (n. mile)	Catch SBW (kg)	Total catch (kg)	% SBW
1	1-Sep-16	Adult	BT	2	51 35.63	169 57.11	456	1.32	112.9	429.4	26
2	1-Sep-16	Imm	BT	2	51 38.46	169 55.58	404	1.73	345.7	538.3	64
3	2-Sep-16	Imm	BT	4	51 49.45	170 18.05	396	0.48	177.2	220.5	80
4	2-Sep-16	Back	BT	3S	51 40.08	170 40.34	478	1.16	52.1	430.8	12
5	3-Sep-16	Back	BT	8N	51 54.25	171 17.11	507	0.85	64.2	347.5	18
6	5-Sep-16	Adult	BT	8S	52 30.51	171 15.06	511	0.95	145.3	357.6	41
7	8-Sep-16	Juv	BT	7S	53 12.71	169 29.45	368	0.55	100.3	214.9	47
8	9-Sep-16	Adult	Camera	7S	53 14.90	170 08.73	450	0.19	-	-	
9	10-Sep-16	Adult	Camera	7S	53 13.52	170 16.68	460	0.14	-	-	
10	11-Sep-16	Juv	BT	7N	52 54.75	170 11.09	349	0.28	22.4	111.1	20
11	11-Sep-16	Imm	BT	7N	52 54.62	170 18.06	418	0.38	104.8	870.4	12
12	11-Sep-16	Adult	MW	8S	52 35.58	171 25.07	400	1.59	0.9	4.1	22
13	12-Sep-16	Adult	BT	8S	52 42.08	171 20.05	466	0.08	190.0	195.7	97
14	12-Sep-16	Adult	Camera	8S	52 42.22	171 21.25	464	0.23	-	-	
15	15-Sep-16	Adult	BT	5	52 25.76	170 19.73	418	0.27	681.3	696.1	98
16	16-Sep-16	Adult	BT	5	52 01.52	170 38.41	418	0.29	201.1	216.3	93
17	16-Sep-16	Juv	BT	4	51 58.93	170 23.97	342	0.30	38.2	80.8	47
18	17-Sep-16	Adult	BT	4	51 44.94	170 33.34	461	0.34	17.0	61.0	28
19	17-Sep-16	Adult	Mooring	4	51 47.17	170 24.53	420	0.20	-	-	
20	17-Sep-16	Adult	BT	4	51 47.05	170 23.24	420	0.60	46.7	96.6	48
21	18-Sep-16	Adult	BT	4	51 47.23	170 23.60	417	0.05	639.1	646.8	99
22	18-Sep-16	Adult	BT	4	51 35.48	170 06.84	469	0.02	169.6	211.8	80
23	19-Sep-16	Meso	BT	2	51 38.92	169 28.67	320	0.24	0.1	0.4	25
24	19-Sep-16	Adult	Camera	4	51 36.33	170 07.47	435	1.11	-	-	
25	20-Sep-16	Adult	BT	4	51 36.38	170 07.16	435	0.08	170.3	173.6	98
Total									3 279.2	5 903.7	56

Table 3: Trawl catch and fish measured during the 2016 acoustic survey of the Campbell Island Rise.

Code	Scientific name	Common name	Catch weight (kg)	Number measured
AMA	*Acesta maui*	*Acesta maui*	4.6	0
ANT	Anthozoa	Anemones	1.3	0
API	*Alertichthys blacki*	Alert pigfish	2.0	24
ASC	Ascidiacea	Sea squirt	0.1	0
BRN	Cirripedia (Class)	Barnacle	0.1	0
BTA	*Brochiraja asperula*	Smooth deepsea skate	1.2	0
BTS	*Brochiraja spinifera*	Prickly deepsea skate	1.4	0
CAM	*Camplyonotus rathbunae*	Sabre prawn	1.0	0
CAS	*Coelorinchus aspercephalus*	Oblique banded rattail	326.0	975
CFA	*Coelorinchus fasciatus*	Banded rattail	22.6	211
COL	*Coelorinchus oliverianus*	Olivers rattail	1.2	49
DCO	*Notophycis marginata*	Dwarf cod	9.0	265
DCS	*Bythaelurus dawsoni*	Dawson's catshark	4.3	7
DDI	*Desmophyllum dianthus*	Desmophyllum dianthus	0.1	0
DSP	*Congiopodus coriaceus*	Deepsea pigfish	10.7	100
ELC	*Electrona carlsbergi*	Carlsberg's lanternfish	0.1	17
ERR	*Errina* spp.	Red coral	0.1	0
GSH	*Hydrolagus novaezealandiae*	Ghost shark	11.1	9
GSP	*Hydrolagus bemisi*	Pale ghost shark	227.2	113
HAK	*Merluccius australis*	Hake	72.9	10
HCO	*Bassanago hirsutus*	Hairy conger	9.4	0
HMT	Hormathiidae	Deepsea anemone	4.2	0
HOK	*Macruronus novaezelandiae*	Hoki	20.5	8
HYA	*Hyalascus* sp.	Floppy tubular sponge	714.9	0
JAV	*Lepidorhynchus denticulatus*	Javelin fish	319.6	953
JFI		Jellyfish	0.4	0
LCH	*Harriotta raleighana*	Long-nosed chimaera	4.2	1
LDO	*Cyttus traversi*	Lookdown dory	11.7	5
LHE	*Lampanyctodes hectoris*	Hector's lanternfish	0.9	122
LIN	*Genypterus blacodes*	Ling	503.2	170
MAN	*Neoachiropsetta milfordi*	Finless flounder	17.4	6
MIQ	*Onykia ingens*	Warty squid	9.7	3
MMU	*Maurolicus australis*	Pearlside	0.1	0
NOS	*Nototodarus sloanii*	NZ southern arrow squid	6.8	7
ONG	Porifera (Phylum)	Sponges	2.2	0
OPA	*Hemerocoetes* spp.	Opalfish	1.3	16
PAM	*Pannychia moseleyi*	*Pannychia moseleyi*	0.1	0
PMO	*Pseudostichopus mollis*	*Pseudostichopus mollis*	1.2	0
PRO	*Protomyctophum spp.*	*Protomyctophum* spp	0.4	126
PYR	*Pyrosoma atlanticum*	*Pyrosoma atlanticum*	2.4	0
RCO	*Pseudophycis bachus*	Red cod	4.0	7
RSK	*Zearaja nasuta*	Rough skate	54.4	22
SAL		Salps	0.6	0
SBW	*Micromesistius australis*	Southern blue whiting	3 279.2	3 765
SCD	*Notothenia microlepidota*	Smallscaled cod	9.2	6
SCO	*Bassanago bulbiceps*	Swollenhead conger	16.2	0
SDF	*Azygopus pinnifasciatus*	Spotted flounder	0.1	1
SMK	*Teratomaia richardsoni*	Spiny masking crab	0.3	0
SPD	*Squalus acanthias*	Spiny dogfish	41.6	21
SSI	*Argentina elongata*	Silverside	145.1	978
TOP	*Ambophthalmos angustus*	Pale toadfish	14.3	7
VNI	*Lucigadus nigromaculatus*	Blackspot rattail	0.6	9
VST	*Neophrynichthys heterospilos*	Variable spotted toadfish	5.5	15
WWA	*Seriolella caerulea*	White warehou	3.8	8
ZOR	*Zoroaster* spp.	Rat-tail star	0.1	0
Total			**5 902.6**	**8 036**

Table 4: Estimates of the ratio *r* used to convert SBW backscatter to biomass. Values are derived from the scaled length frequency distributions in Figure 8. Abundance estimates (Table 6) were calculated using *r* from commercial tows for adult SBW in the southern and eastern areas, and from research tows for juvenile and immature SBW, and for adult SBW in the northern area where there was little commercial fishing. σ is the acoustic backscattering coefficient.

Category	Data source	No. of trawls measured	Mean length (cm)	Mean weight (g)	Mean σ (m^2)	Mean TS (dB)	*r* ($kg\ m^{-2}$)
Adult (north)	Commercial	4	37.0	372	0.000408	-33.9	912
Adult (east)	Commercial	91	38.6	427	0.000450	-33.5	950
Adult (south)	Commercial	95	39.0	446	0.000462	-33.4	964
Adult (all)	Commercial	190	38.8	437	0.000456	-33.4	958
Adult (north)	Research	10	35.3	329	0.000372	-34.3	883
Adult (east)	Research	4	38.1	410	0.000437	-33.6	939
Immature	Research	3	27.1	138	0.000204	-36.9	675
Juvenile	Research	3	15.6	26	0.000062	-42.1	425

Table 5: Gonad stages of SBW caught in research trawls during the 2016 acoustic survey. Gonad stages are defined in Appendix 4.

				Males							Females						
Tow	Date	Stratum	Mark type	1	2	3	4	5	6	7	1	2	3	4	5	6	7
1	1-Sep-16	2	Adult	2	0	12	43	3	0	0	3	0	174	10	5	0	0
2	1-Sep-16	2	Imm	65	20	33	7	0	0	0	133	2	5	1	0	0	0
3	2-Sep-16	4	Imm	74	10	25	0	0	0	0	105	1	0	0	0	0	0
4	2-Sep-16	3S	Back	1	1	39	3	4	0	0	5	0	93	5	1	0	0
5	3-Sep-16	8N	Back	0	0	11	30	1	0	0	1	0	89	2	0	0	0
6	5-Sep-16	8S	Adult	6	2	30	8	30	0	0	7	2	143	4	2	0	0
7	8-Sep-16	7S	Juv	103	11	4	0	0	0	0	136	0	1	0	0	0	0
10	11-Sep-16	7N	Juv	6	0	2	0	0	0	0	17	0	0	0	0	0	0
11	11-Sep-16	7N	Imm	91	0	14	0	1	0	0	90	1	0	1	0	0	0
12	11-Sep-16	8S	Adult	0	0	0	0	0	1	0	0	0	0	0	0	0	2
13	12-Sep-16	8S	Adult	0	0	4	2	33	50	6	0	1	10	3	6	70	31
15	15-Sep-16	5	Adult	4	0	2	1	22	41	36	5	0	16	4	11	42	48
16	16-Sep-16	5	Adult	34	7	4	0	2	7	24	74	2	0	0	0	11	60
17	16-Sep-16	4	Juv	85	0	0	0	0	0	0	110	0	0	0	0	0	0
18	17-Sep-16	4	Adult	1	1	0	0	1	10	22	1	1	0	3	3	3	1
20	17-Sep-16	4	Adult	3	0	1	0	25	25	39	3	0	8	7	14	8	29
21	18-Sep-16	4	Adult	20	1	2	0	33	40	26	27	1	4	17	19	13	49
22	18-Sep-16	4	Adult	3	1	15	1	22	11	52	2	0	27	10	48	10	18
23	19-Sep-16	2	Meso	0	0	1	0	0	0	0	0	0	0	0	0	0	0
25	20-Sep-16	4	Adult	1	0	0	1	10	16	54	1	0	2	2	1	40	78

Table 6: Abundance estimates (t) and CV by stratum and snapshot of immature and adult SBW for the Campbell Island Rise in 2016.

	Juvenile		Immature		Adult	
Stratum	Biomass (t)	CV	Biomass (t)	CV	Biomass (t)	CV
Snapshot 1						
2	0	–	1 094	40	7 477	57
3N	0	–	0	–	0	–
3S	0	–	0	–	0	–
4	0	–	2 184	34	8 082	70
5	0	–	910	83	0	–
6N	0	–	0	–	0	–
6S	0	–	0	–	0	–
7N	0	–	1 720	47	0	–
7S	624	68	345	68	6 861	70
8E	0	–	0	–	588	100
8N	0	–	0	–	0	–
8S	0	–	0	–	3 780	100
Total	624	68	6 252	23	26 788	35
Snapshot 2						
2	206	101	0	–	11 891	61
3N	0	–	0	–	0	–
3S	0	–	0	–	0	–
4	141	63	329	78	21 467	28
5	261	104	1 505	50	12 393	16
6N	0	–	0	–	1 226	100
6S	0	–	0	–	2 583	81
7N	318	49	778	67	636	98
7S	0	–	47	100	8 347	58
8E	0	–	0	–	7 471	45
8N	0	–	0	–	0	–
8S	0	–	0	–	47 260	28
Total	926	42	2 660	36	113 274	16
Average	775	37	4 456	19	70 031	14

Table 7: Biomass estimates (t) by survey and category for the Campbell Island Rise. Values for surveys from 1993–2011 are from Fu et al. (2013) and all were calculated using estimates of TS from O'Driscoll et al. (2013).

	Juvenile	CV	Immature	CV	Adult	CV
1993	0	–	35 208	25	16 060	24
1994	0	–	8 018	38	72 168	34
1995	0	–	15 507	29	53 608	30
1998	322	45	6 759	20	91 639	14
2000	423	39	1 864	24	71 749	17
2002	1 969	39	247	76	66 034	68
2004	639	67	5 617	16	42 236	35
2006	504	38	3 423	24	43 843	32
2009	0	–	24 479	26	99 521	27
2011	0	–	14 454	17	53 299	22
2013	0	–	8 004	55	65 801	25
2016	775	37	4 456	19	97 117	16

8. FIGURES

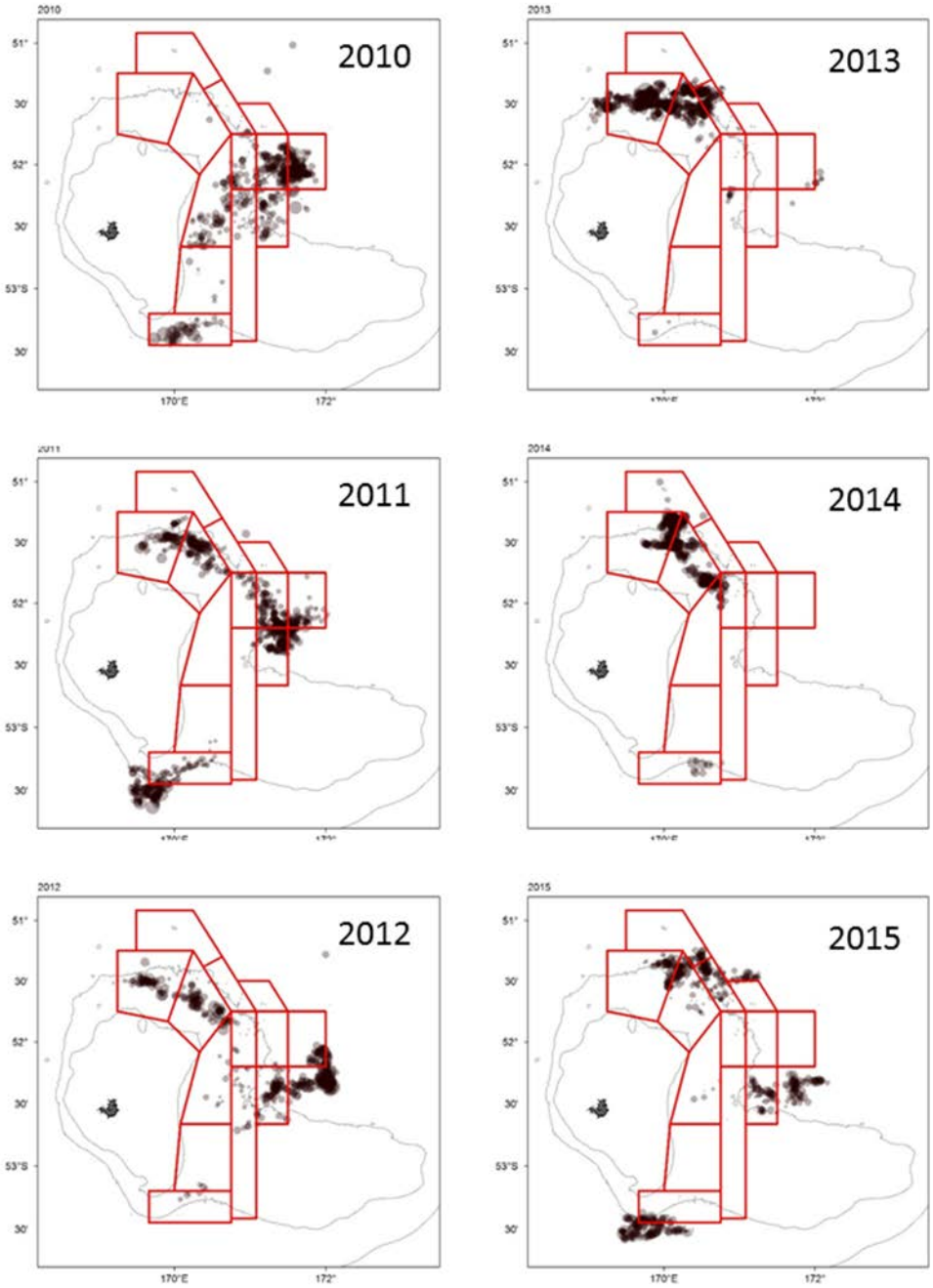

Figure 1: Stratum boundaries for Snapshot 1 of 2013 acoustic survey superimposed on plots of catch rates from commercial trawls on the Campbell Island Rise from 2010–15. Circle area is proportional to SBW catch rate.

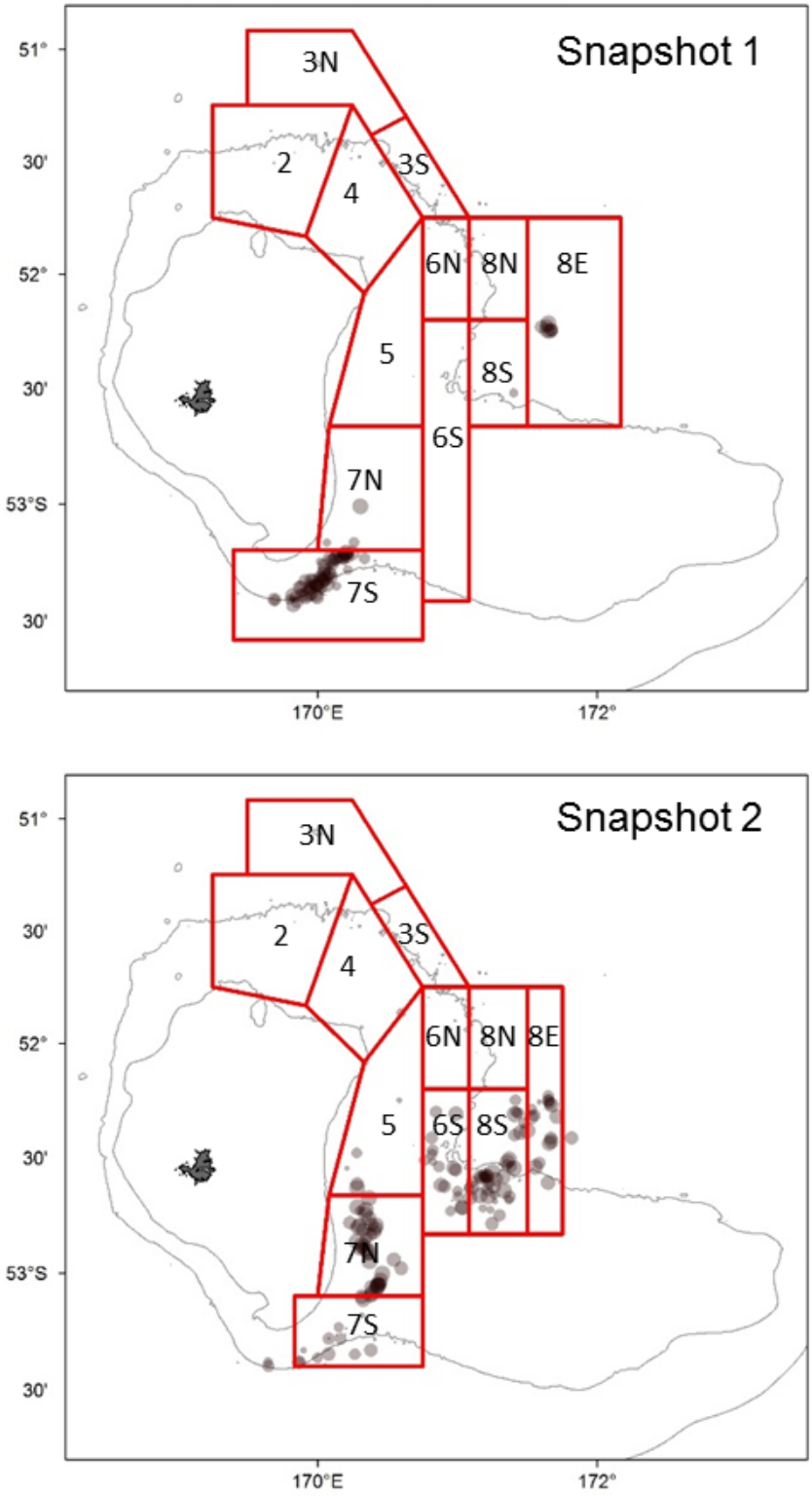

Figure 2: Stratum boundaries for snapshot 1 (upper panel) and snapshot 2 (lower panel) of the 2016 acoustic survey of the Campbell Island Rise superimposed on plots of catch rates from commercial trawls carried out during each snapshot (31 August – 10 September for snapshot 1, 11–20 September for Snapshot 2). Circle area is proportional to SBW catch rate. Strata 2–7 are the core acoustic strata which have been covered in all previous surveys.

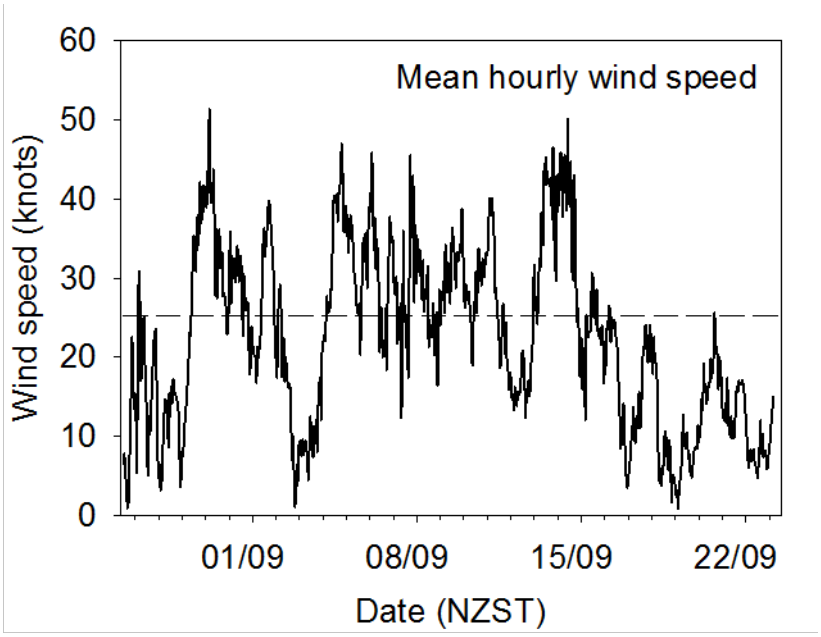

Figure 3: Output from *Tangaroa* data acquisition system (DAS) showing mean hourly wind speed (in knots) during the survey. Data are true wind speed, i.e., corrected for relative motion of ship.

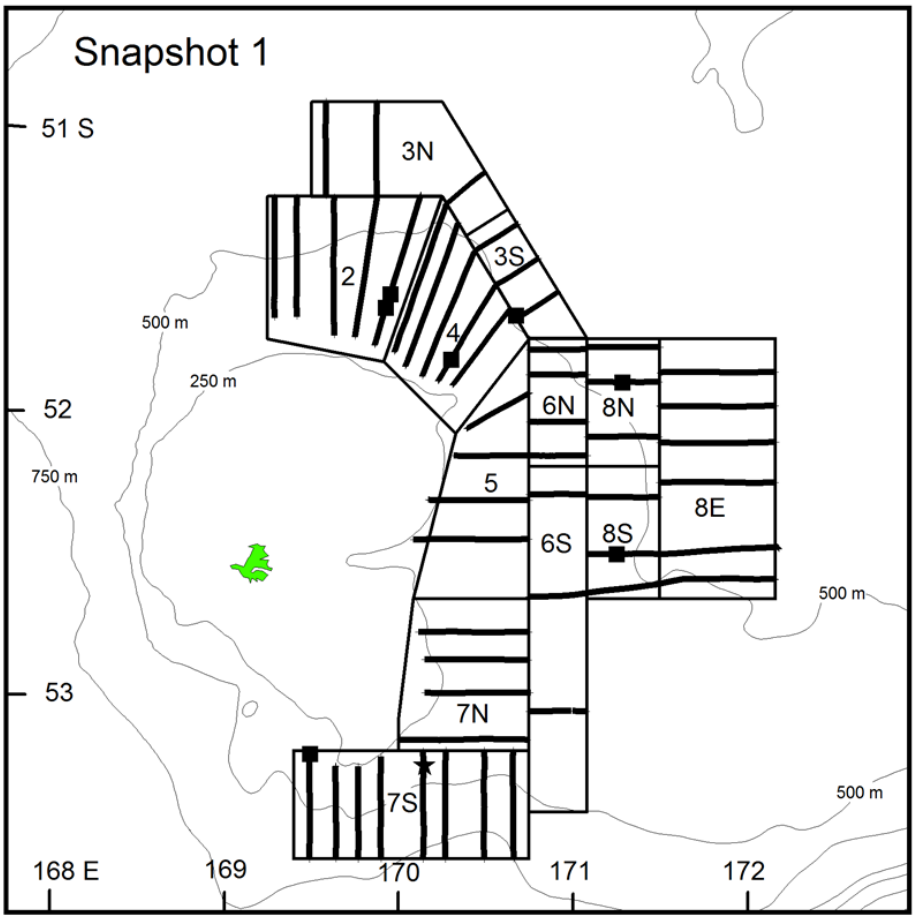

Figure 4: Location of stratum boundaries, acoustic transects (black lines), and sampling stations during snapshot 1 on 31 August to 10 September 2016. Squares are bottom trawls, and stars are camera drops.

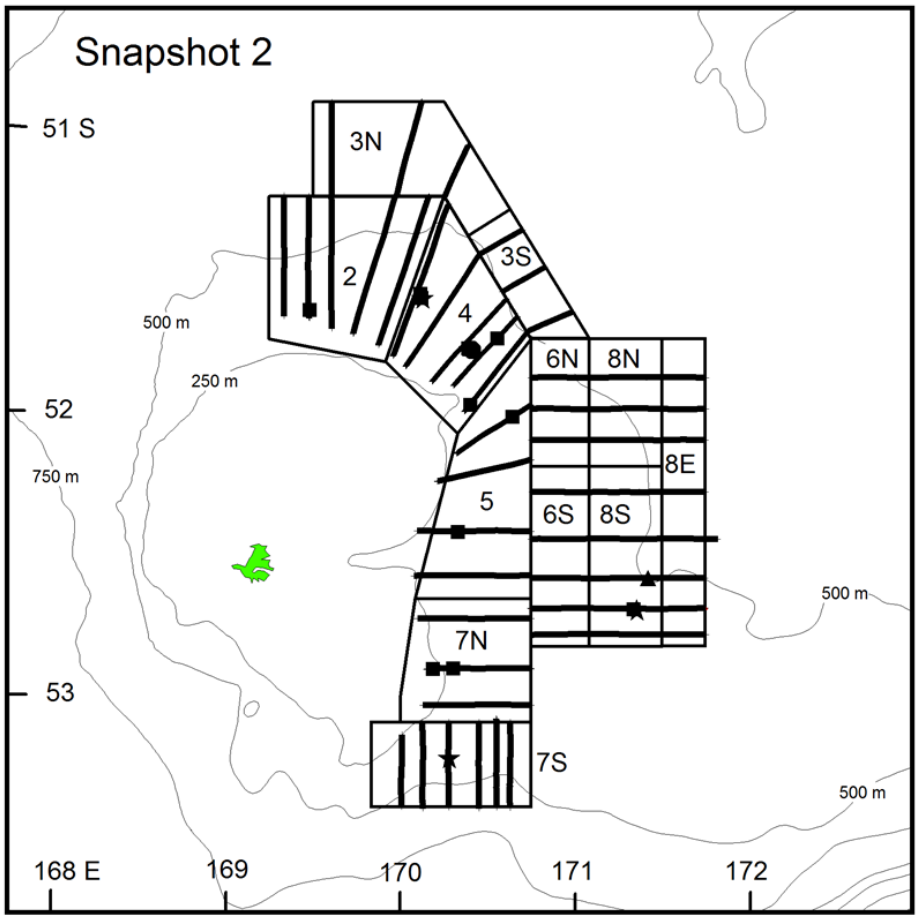

Figure 5: Location of stratum boundaries, acoustic transects (black lines), and sampling stations during snapshot 2 on 10–20 September 2016. Squares are bottom trawls, triangles are midwater trawls, stars are camera drops, and circle is camera mooring.

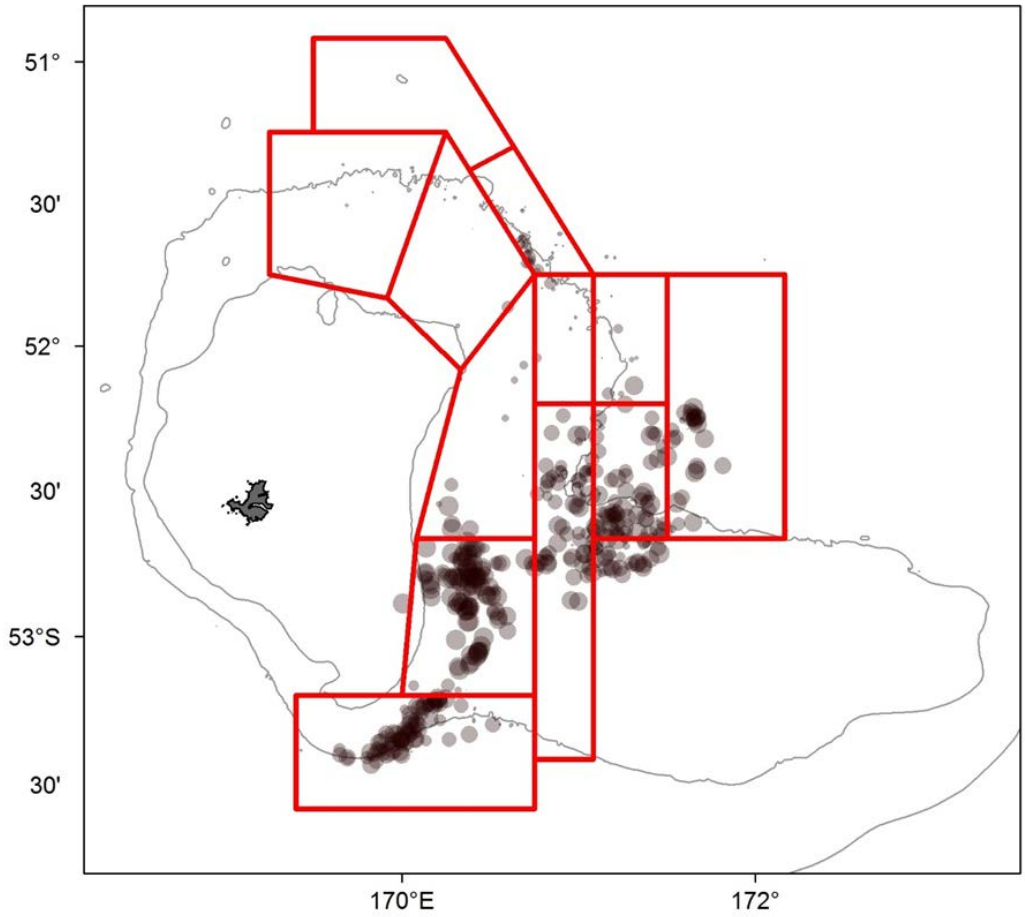

Figure 6: Commercial catch rates of SBW in 2016 Campbell Island fishery. Snapshot 1 stratum boundaries are shown in red. Circle area is proportional to SBW catch rate.

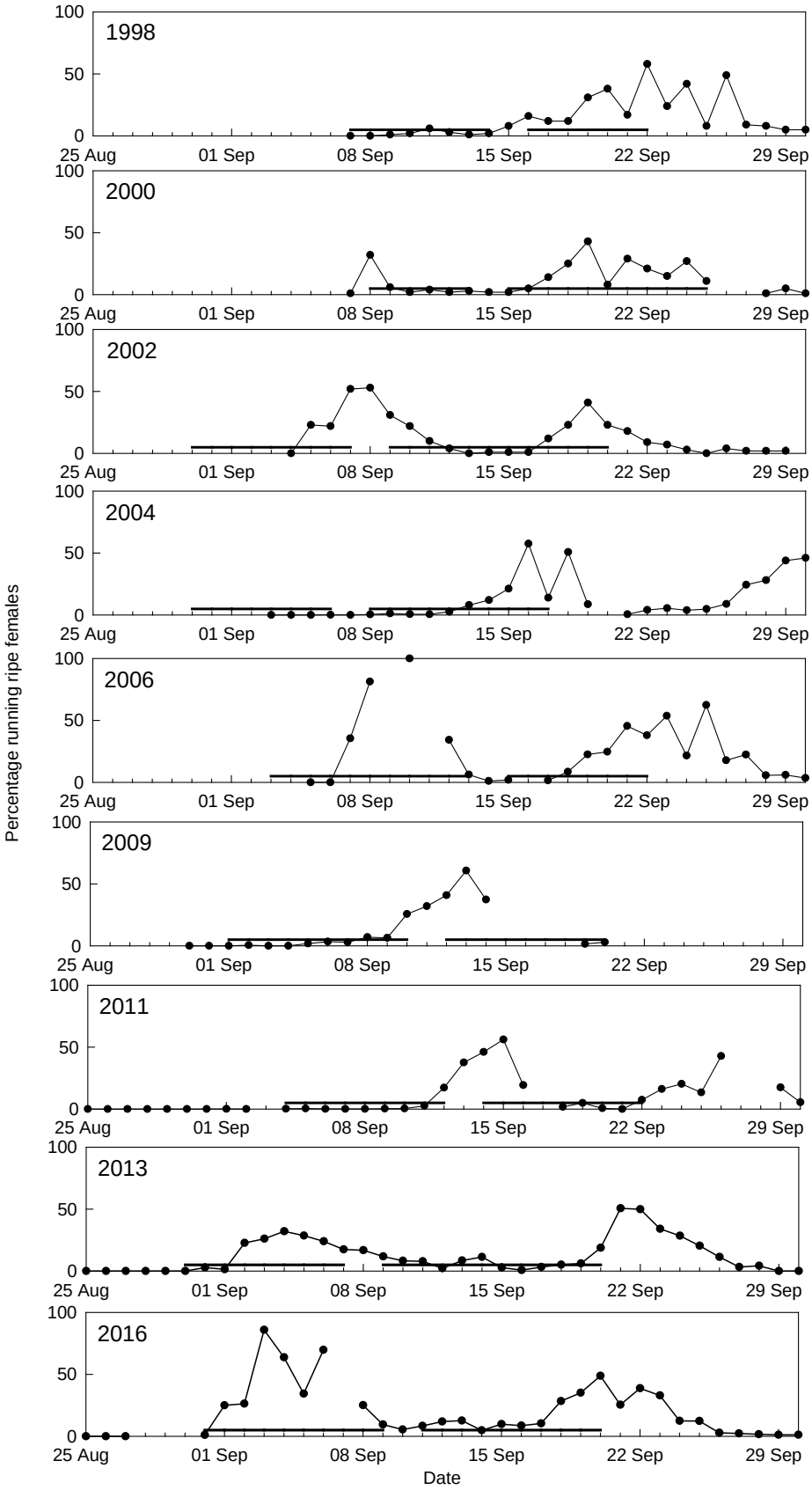

Figure 7: Survey timing (line above x axis) in relation to the timing of spawning for the acoustic surveys from 1998 to 2016 on the Campbell Island Rise. Percentage of running ripe females is from observer data.

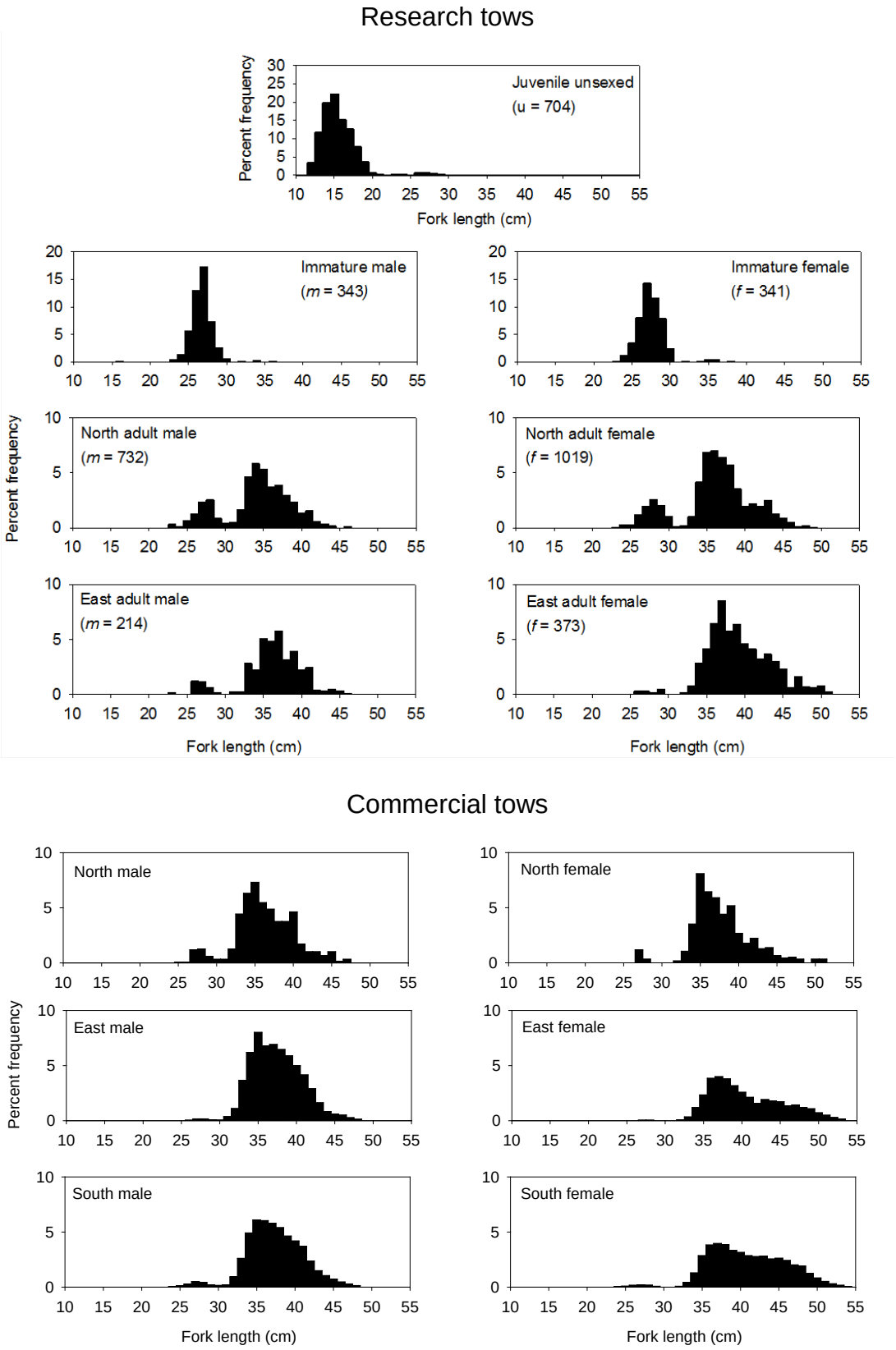

Figure 8: Catch-weighted length frequency distributions for southern blue whiting caught in research trawls by *Tangaroa* from juvenile, immature and adult marks, and from commercial tows during the spawning fishery. Size distributions for adults were separated into northern, eastern, and southern areas. *m* and *f* values for research tows show number of males and females measured.

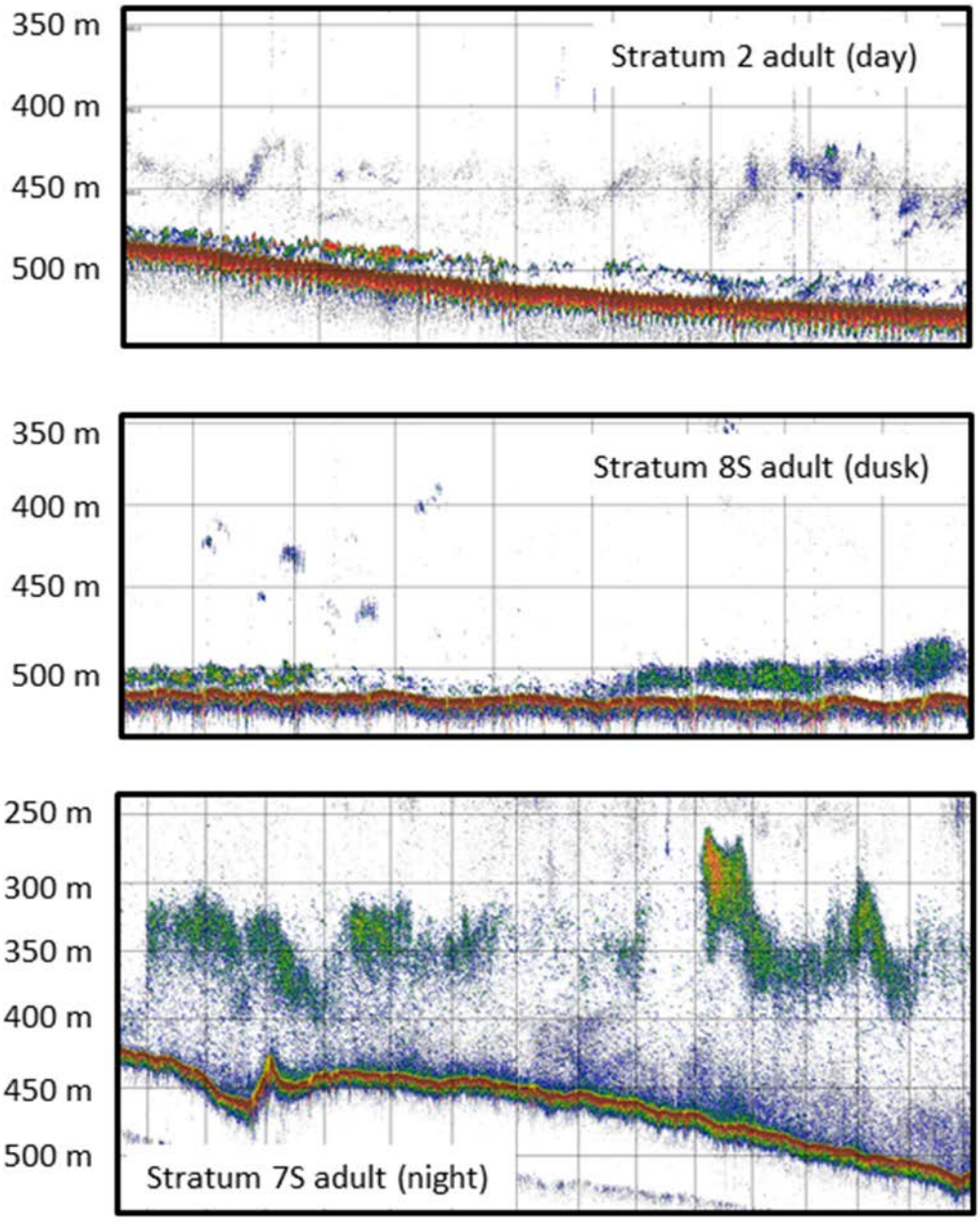

Figure 9: Examples of echograms showing pre-spawning adult SBW marks during snapshot 1. Each gridded cell is 0.5 nautical miles horizontally by 50 m vertically.

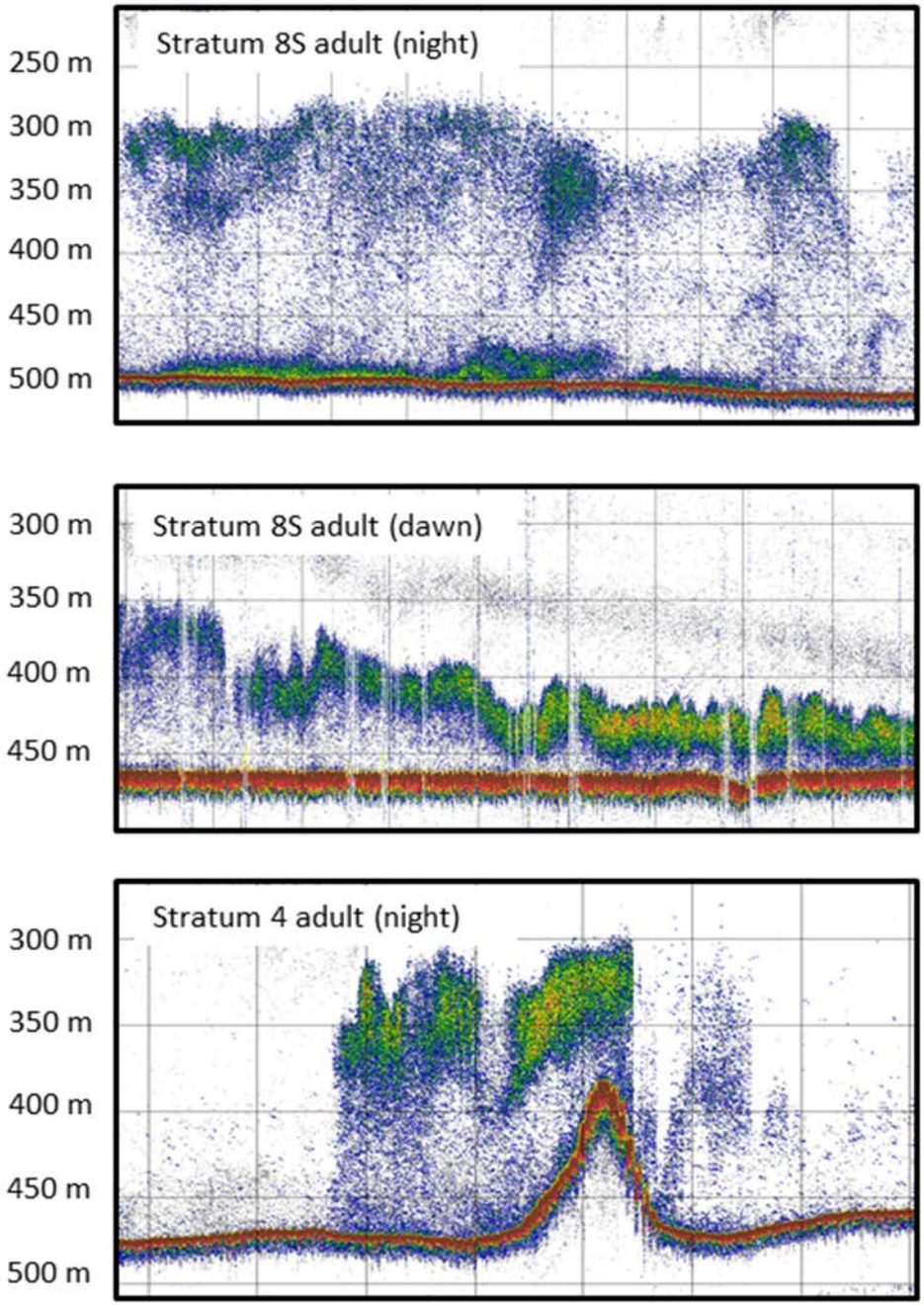

Figure 10: Examples of echograms showing post-spawning adult SBW marks during snapshot 2. Each gridded cell is 0.5 nautical miles horizontally by 50 m vertically.

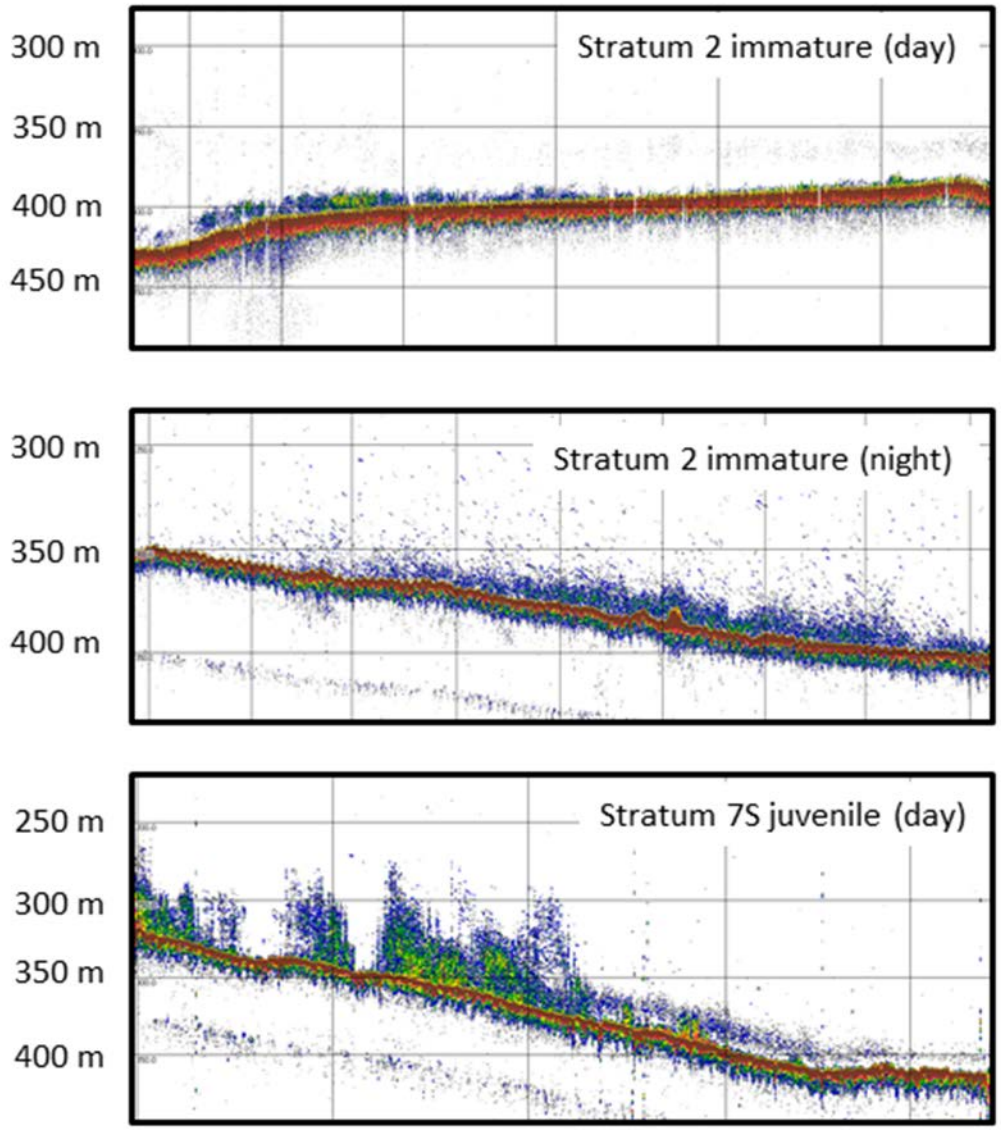

Figure 11: Examples of echograms showing immature and juvenile SBW marks. Each gridded cell is 0.5 nautical miles horizontally by 50 m vertically.

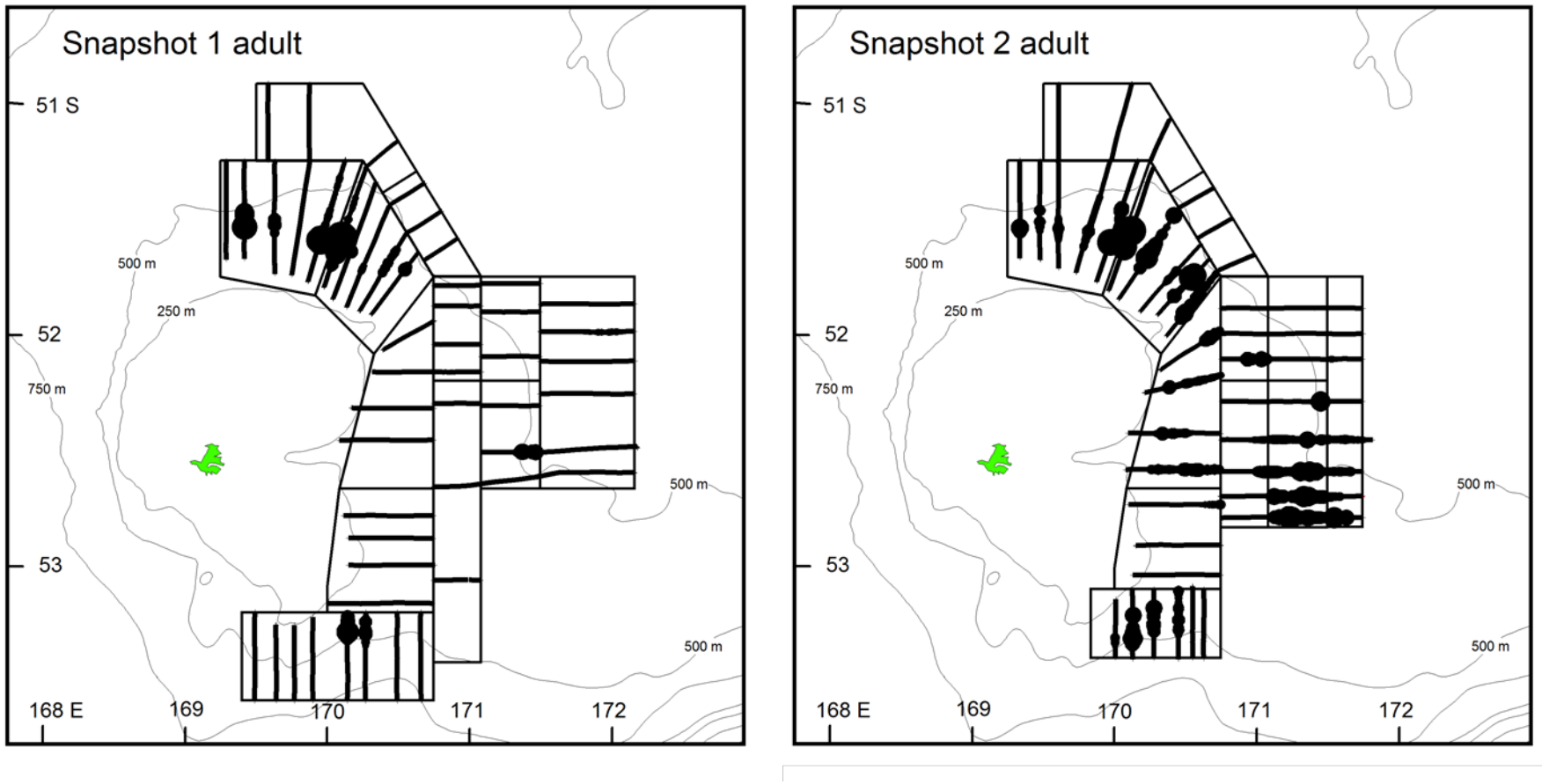

Figure 12: Spatial distribution of acoustic backscatter from adult SBW plotted in 10 ping (approximately 100 m) bins for snapshots 1 and 2. Circle area is proportional to the log of the acoustic backscatter.

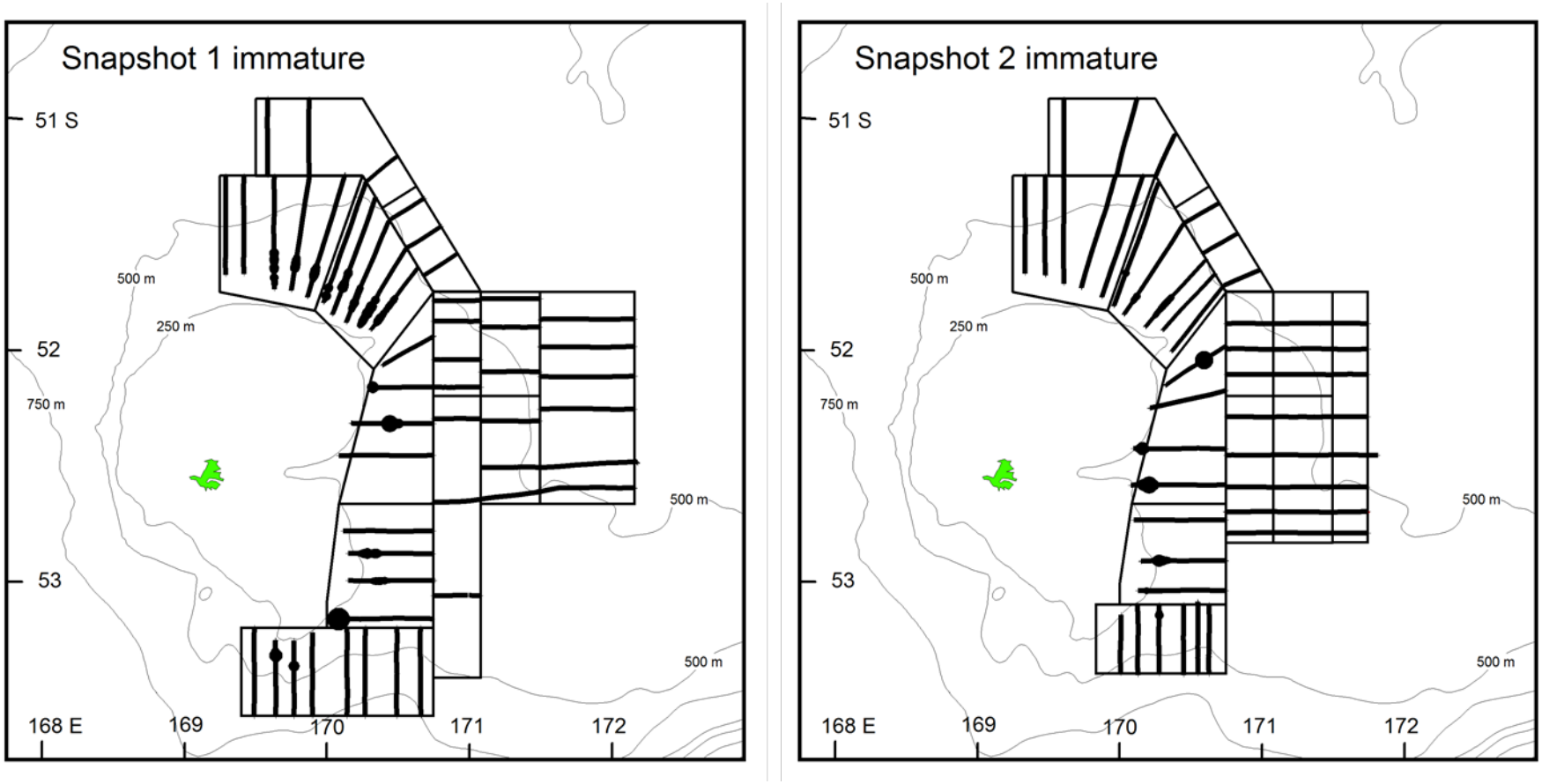

Figure 13: Spatial distribution of acoustic backscatter from immature SBW plotted in 10 ping (approximately 100 m) bins for snapshots 1 and 2. Circle area is proportional to the log of the acoustic backscatter.

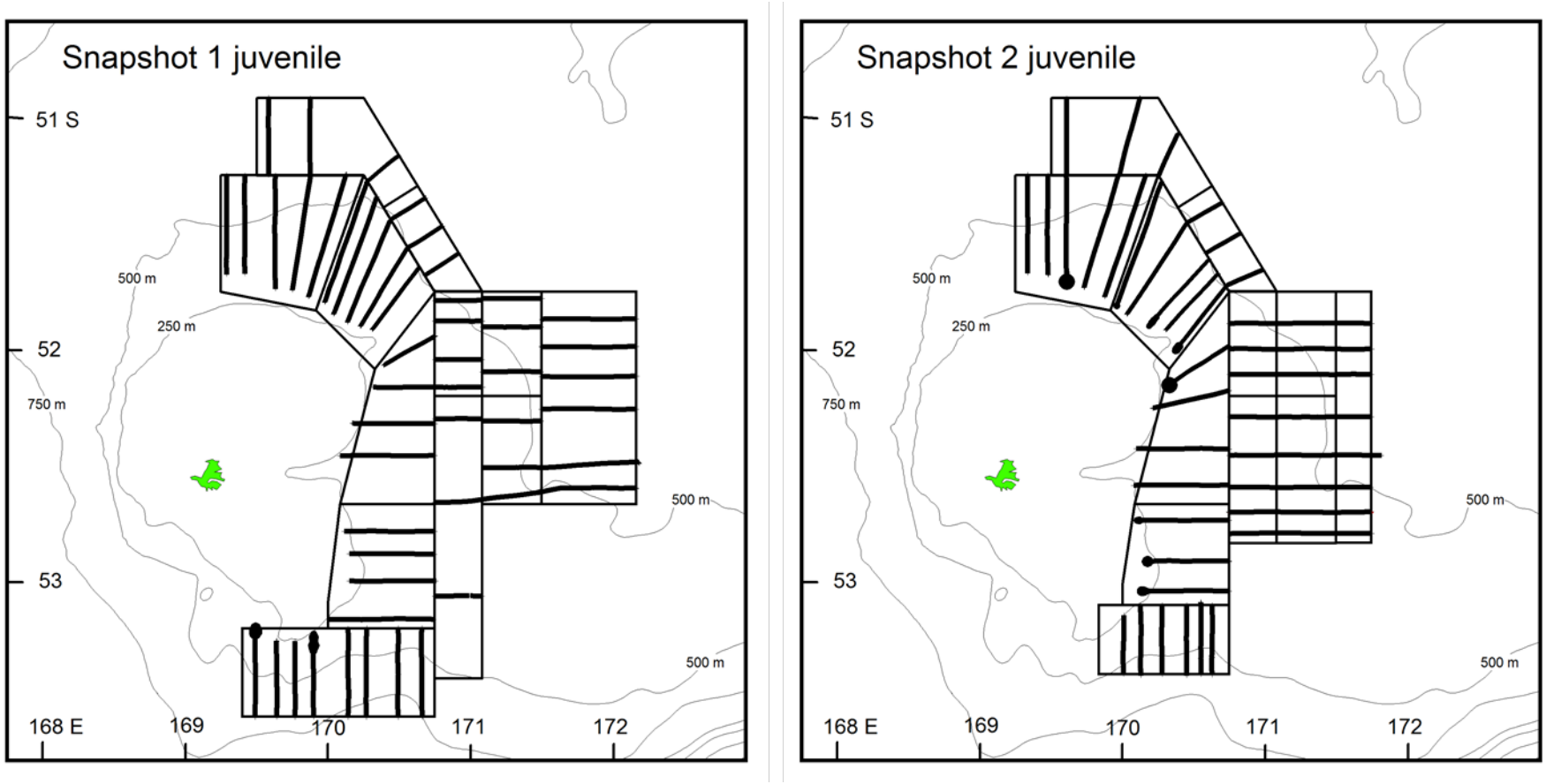

Figure 14: Spatial distribution of acoustic backscatter from juvenile SBW plotted in 10 ping (approximately 100 m) bins for snapshots 1 and 2. Circle area is proportional to the log of the acoustic backscatter.

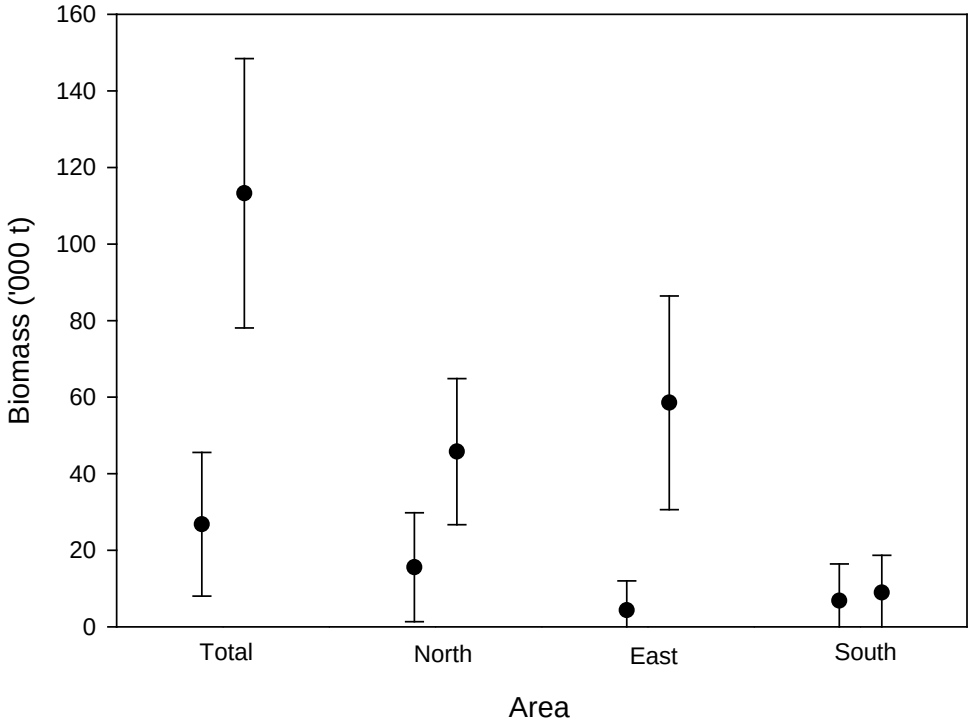

Figure 15: Comparison of snapshot 1 and 2 biomass estimates for adult SBW by area for the 2016 Campbell acoustic survey. Error bars are ± 2 standard errors. Estimates by strata are given in Table 6.

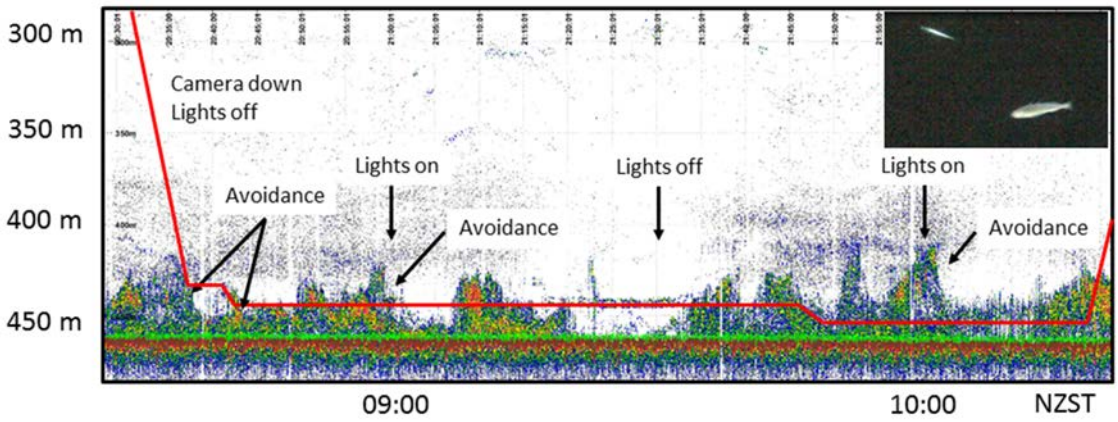

Figure 16: Annotated echogram collected during camera deployment at station 14 in stratum 8S during day on 12 September. The position of the camera is shown by the red line, and the times at which lights turned on and off and fish reaction noted. Inset shows image of SBW from video.

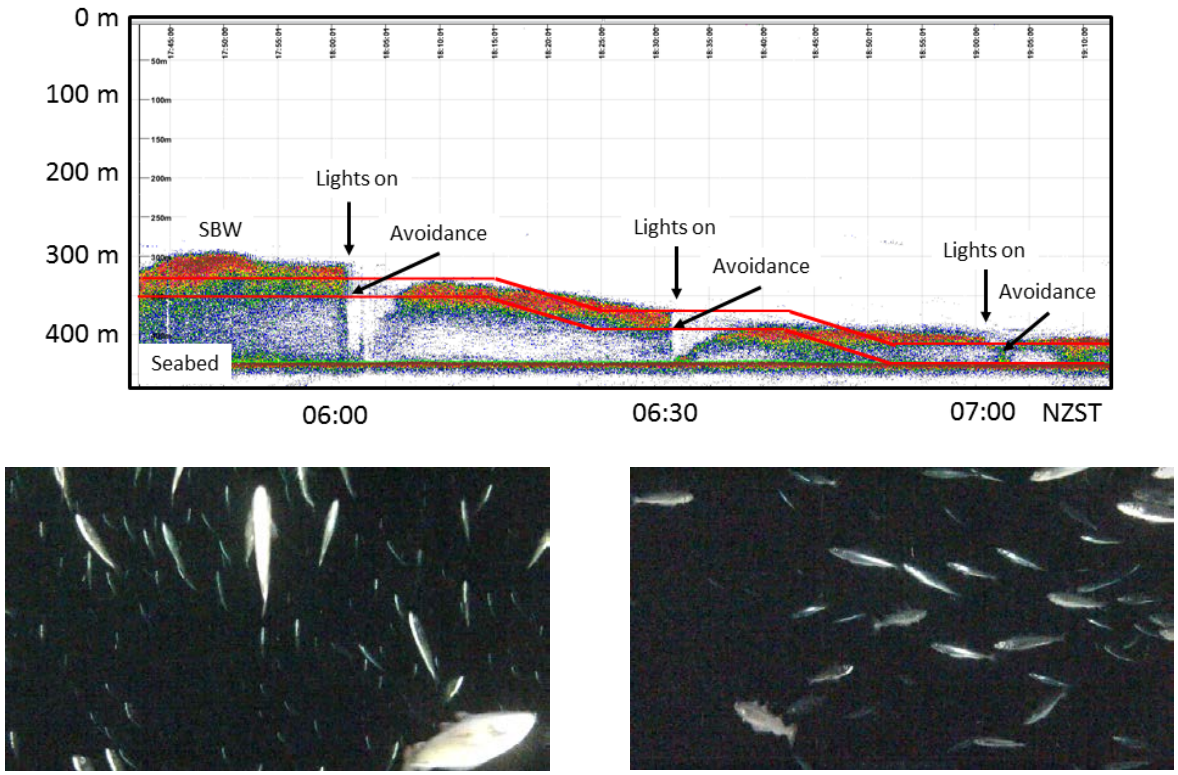

Figure 17: Annotated echogram collected during camera deployment at station 24 in stratum 4 at dawn on 20 September. The positions of the cameras are shown by the red lines, and the times at which lights turned on and fish reaction noted. Lights stayed on for 2 minutes every 30 minutes. The cameras were lowered on the winch to follow the fish as they descended. Lower panels show images of SBW from video recorded by the top camera.

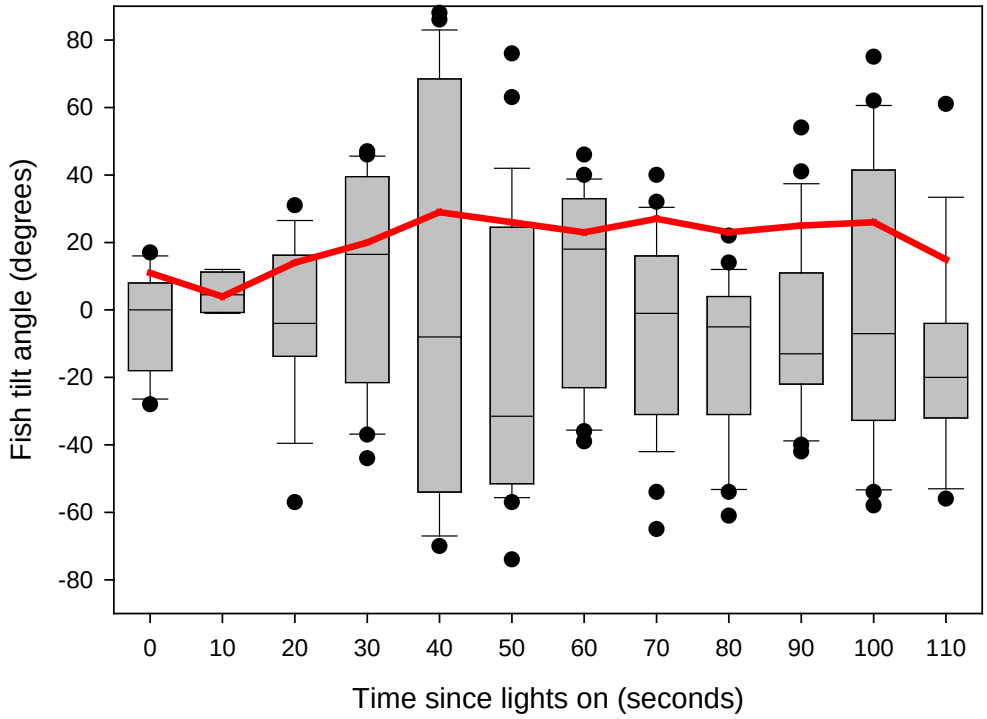

Figure 18: Measured tilt angle distribution (box and whiskers plot) of SBW observed *in situ* on moored and lowered cameras relative to the time since lights turned on. Boxes show 25th and 75th quartiles separated by the median, with whiskers between 10th and 90th percentile and outliers shown as dots. Red line shows the number of fish measured at each time step.

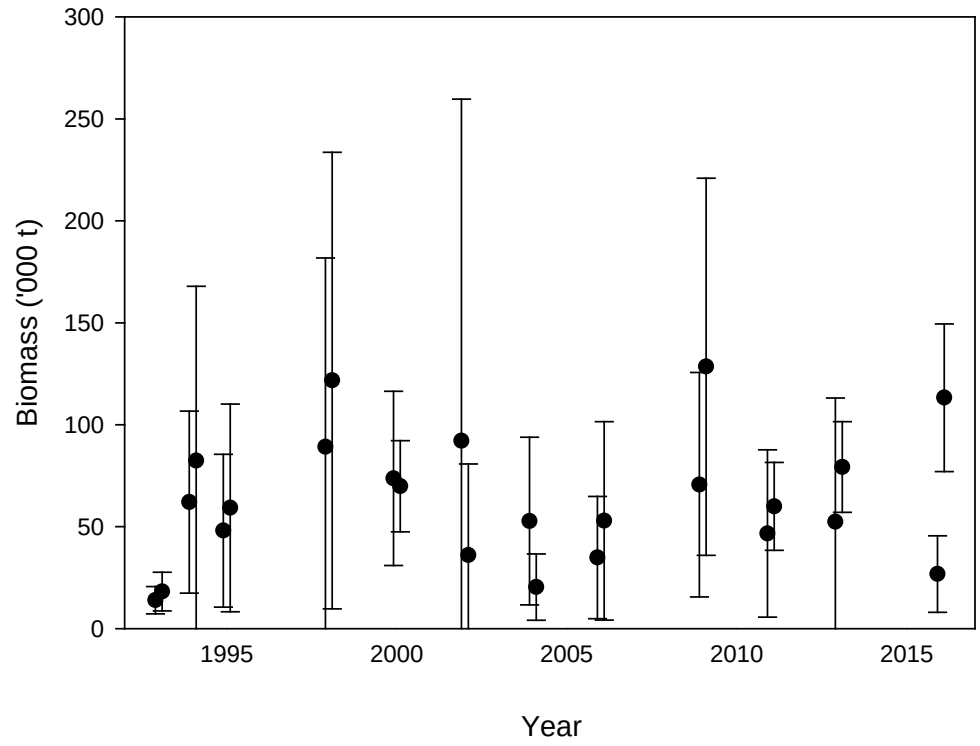

Figure 19: Comparison of snapshot 1 and 2 biomass estimates for adult SBW for all Campbell acoustic surveys. Error bars are ± 2 standard errors. Values for surveys from 1993–2011 are from Fu et al. (2013) and all were calculated using estimates of TS from O'Driscoll et al. (2013).

APPENDIX 1: Calibration of *Tangaroa* hull echosounders

The 18, 38, 70, 120, and 120 kHz EK60 echosounders on *Tangaroa* were calibrated on 27 August 2016 in East Bay, Marlborough Sounds (41˚ 09.4' S, 174˚ 20.1' E), at the start of the Campbell southern blue whiting acoustic survey (TAN1610). The calibration was conducted broadly according to the procedures in Demer et al. (2015).

We used divers to minimise set-up time. New Zealand Diving Services provided dive support from their vessel Topside. Bruce Lines was the chief diver. The calibration started at 10:30 NZST. The sphere and associated lines were immersed in a soap solution prior to entering the water. A lead weight was also deployed about 3 m below the sphere to steady the arrangement of lines. The diver attached the lines, and made sure that these were not fouled. Long (3.8 m) fibreglass calibration poles were used to help keep the calibration lines clear of the hull.

The weather during the calibration was fair, with 20–25 knots of westerly wind, no swell, and a 0.5 m chop. The vessel was anchored but swinging at 0.3–0.7 knots. Water depth was about 45 m.

The sphere was located in the beam immediately at 10:40, and the divers and support boat returned to port at 11:30. The sphere was first centred in the beam of the 38 kHz transducer to obtain data for the on-axis calibration. It was then moved around to obtain data for the beam shape calibration. Due to the close proximity of all five transducers, a number of echoes were recorded across all frequencies. After the 38 kHz calibration, the sphere was moved to ensure on-axis calibration of the other frequencies.

The calibration data were recorded in one EK60 raw format file (tan1610-D20160826-T224922.raw). These data are stored in the NIWA *acoustics* database. The EK60 transceiver settings in effect during the calibration are given in Table A1.1.

A temperature/salinity/depth profile was taken using a Seabird SBE21 conductivity, temperature, and depth probe (CTD). Estimates of acoustic absorption were calculated using the formulae in Doonan et al. (2003). The formula from Francois & Garrison (1982) was used at 200 kHz. Estimates of seawater sound speed and density were calculated using the formulae of Fofonoff & Millard (1983). The sphere target strength was calculated as per equations 6 to 9 in MacLennan (1981), using longitudinal and transverse sphere sound velocities of 6853 and 4171 m s^{-1} respectively and a sphere density of 14 900 kg m^{-3}.

Analysis

The data in the .raw EK60 files were extracted using custom-written software. The amplitude of the sphere echoes was obtained by filtering on range, and choosing the sample with the highest amplitude. Instances where the sphere echo was disturbed by fish echoes were discarded. The alongship and athwartship beam widths and offsets were calculated by fitting the sphere echo amplitudes to the Simrad theoretical beam pattern:

$$compensation = 6.0206\left(\left(\frac{2\theta_{fa}}{BW_{fa}}\right)^2 + \left(\frac{2\theta_{ps}}{BW_{ps}}\right)^2 - 0.18\left(\frac{2\theta_{fa}}{BW_{fa}}\right)^2\left(\frac{2\theta_{ps}}{BW_{ps}}\right)^2\right),$$

where θ_{ps} is the port/starboard echo angle, θ_{fa} the fore/aft echo angle, BW_{ps} the port/starboard beamwidth, BW_{fa} the fore/aft beamwidth, and *compensation* the value, in dB, to add to an uncompensated echo to yield the compensated echo value. The fitting was done using an unconstrained nonlinear optimisation (as implemented by the Matlab fminsearch function). The S_a correction was calculated from:

$$Sa, corr = 5\log 10\left(\frac{\sum P_i}{4P_{\max}}\right),$$

where P_i is sphere echo power measurements and P_{max} the maximum sphere echo power measurement. A value for $S_{a,corr}$ is calculated for all valid sphere echoes and the mean over all sphere echoes is used to determine the final $S_{a,corr}$.

Results

The results from the CTD cast are given in Table A1.2, along with estimates of the sphere target strength, sound speed, and acoustic absorption for 18, 38, 70, 120, and 200 kHz.

The calibration parameters resulting from the calibration are given in Table A1.3, and compared with results from previous calibrations. Results for all frequencies have been relatively consistent (usually within 0.5 dB) across all calibrations, with higher frequencies (70, 120, and 200 kHz) being more variable over time. The new 38 kHz transducer has slightly higher estimated gain than the previous one.

The estimated beam patterns, as well as the coverage of the beam by the calibration sphere, are given in Figures A1.1–A1.10. The symmetrical nature of the beam patterns and the centering near zero indicates that the transducers and EK60 transceivers were all operating correctly. The new 38 kHz transducer (fitted in October 2015) had very similar calibration values to those recorded in February 2016, with no indication of the slight estimated beam offset recorded in that calibration (see Table A1.3).

The root mean square (RMS) of the difference between the Simrad beam model and the sphere echoes out to the 3 dB beamwidth was 0.10 dB for 18 kHz, 0.11 for 38 kHz, 0.13 dB for 70 kHz, 0.17 dB for 120 kHz, and 0.19 dB at 200 kHz (Table A1.3), indicating excellent quality calibrations on all frequencies (<0.4 dB is acceptable, <0.3 dB good, and <0.2 dB excellent). On-axis estimates were derived from 564 sphere echoes at 18 kHz, 391 echoes at 38 kHz, 271 echoes at 70 kHz, 39 echoes at 120 kHz, and 245 echoes at 200 kHz. These were much larger sample sizes of on-axis echoes than were recorded during the February 2016 calibration (when fewer than 10 on-axis echoes were recorded at 70, 120, and 200 kHz).

Table A1.1: EK60 transceiver settings and other relevant parameters in effect during the calibration. These were derived from the May 2008 calibration (see Table A1.3).

Parameter					
Frequency (kHz)	18	38	70	120	200
GPT model	00907205c476	0090720580ea	00907205ca98	009072058148	00907205da23
GPT serial number	652	650	674	668	692
GPT software version	050112	050112	050112	050112	050112
ER60 software version	2.4.3	2.4.3	2.4.3	2.4.3	2.4.3
Transducer model	ES18-11	ES38B	ES70-7C	ES120-7C	ES200-7C
Transducer serial number	2080	31378	158	477	364
Sphere type/size			tungsten carbide/38.1 mm diameter (same for all frequencie		
Transducer draft setting (m)	0.0	0.0	0.0	0.0	0.0
Transmit power (W)	2000	2000	750*	250*	150*
Pulse length (ms)	1.024	1.024	1.024	1.024	1.024
Transducer peak gain (dB)	22.96	25.81	26.43	26.17	24.96
Sa correction (dB)	-0.81	-0.57	-0.35	-0.36	-0.25
Bandwidth (Hz)	1574	2425	2859	3026	3088
Sample interval (m)	0.191	0.191	0.191	0.191	0.191
Two-way beam angle (dB)	–17.0	–20.6	–21.0	–21.0	–20.7
Absorption coefficient (dB/km)	2.7	9.8	22.8	37.4	52.7
Speed of sound (m/s)	1494	1494	1494	1494	1494
Angle sensitivity (dB) along/athwartship	13.90/13.90	21.90/21.90	23.0/23.0	23.0/23.0	23.0/23.0
3 dB beamwidth (º) along/athwartship	10.8/10.8	7.0/7.0	6.6/6.6	6.5/6.6	6.8/6.9
Angle offset (º) along/athwartship	0.0/0.0	0.0/0.0	0.0/0.0	0.0/0.0	0.0/0.0

* Maximum transmit power of 70, 120, and 200 kHz echosounders was reduced when ER60 software was upgraded in April 2013. Previously transmit power was 1000 W, 500 W, and 300 W respectively.

Table A1.2: CTD cast details and derived water properties. The values for sound speed, salinity and absorption are the mean over water depths 6 to 30 m.

Parameter	
Date/time (NZST, start)	27 Aug 2016 14:07
Position	41˚ 09.34’ S, 174˚ 20.01’ E
Mean sphere range (m)	24.1 (18 kHz), 24.0 (38), 24.0 (70), 23.9 (120), 24.0 (200)
Mean temperature (ºC)	11.8
Mean salinity (psu)	35.0
Sound speed (m/s)	1496.3
Water density (kg/m^3)	1026.7
Sound absorption (dB/km)	2.39 (18 kHz)
	9.30 (38 kHz)
	22.86 (70 kHz)
	39.31 (120 kHz)
	57.97 (200 kHz)
Sphere target strength (dB re 1m^2)	–42.65 (18 kHz)
	–42.41 (38 kHz)
	–41.39 (70 kHz)
	–39.50 (120 kHz)
	–39.12 (200 kHz)

Table A1.3: Estimated calibration coefficients for all calibrations of *Tangaroa* hull EK60 echosounders. Transducer peak gain was estimated from mean sphere TS. * The 38 kHz transducer was changed in October 2015. The Feb 2015 calibration was in Antarctica.

		Aug 2016	Feb 2016	Feb 2015	Jul 2013	Jul 2012	Feb 2012	Aug 2011	Jan 2010	May 2008
18 kHz										
	Transducer peak gain (dB)	22.80	22.85	23.21	22.99	22.97	22.81	22.78	23.36	22.96
	Sa correction (dB)	-0.71	-0.73	-0.76	-0.78	-0.84	-0.69	-0.69	-0.76	–0.81
	Beamwidth (º) along/athwartship	10.6/10.9	10.5/11.3	10.7/11.2	10.6/10.7	10.7/11.2	10.7/10.9	10.9/11.1	11.1/11.3	10.8/10.8
	Beam offset (º) along/athwartship	0.00/0.00	0.00/0.00	0.00/0.00	0.00/-0.00	0.00/-0.00	0.00/-0/.00	-0.02/0.08	0.00/0.00	0.00/0.00
	RMS deviation (dB)	0.10	0.14	0.12	0.08	0.09	0.14	0.08	0.14	0.26
38 kHz*										
	Transducer peak gain (dB)	26.23	26.21	25.69	25.42	25.62	25.75	25.75	25.98	25.81
	Sa correction (dB)	-0.62	-0.58	-0.54	-0.55	-0.61	-0.57	-0.58	-0.58	–0.57
	Beamwidth (º) along/athwartship	7.0/7.1	6.9/7.2	6.8/6.9	6.8/6.9	6.8/6.9	6.8/6.8	6.8/6.9	6.9/7.0	7.0/7.0
	Beam offset (º) along/athwartship	0.00/0.00	0.14/-0.19	0.00/0.00	0.00/0.00	0.00/0.00	0.00/0.00	0.00/0.00	0.00/0.00	0.00/0.00
	RMS deviation (dB)	0.11	0.14	0.12	0.09	0.10	0.14	0.08	0.10	0.16
70 kHz										
	Transducer peak gain (dB)	26.33	26.28	26.55	26.43	26.04	26.78	26.23	26.78	26.43
	Sa correction (dB)	-0.31	-0.38	-0.35	-0.37	-0.31	-0.35	-0.32	-0.30	–0.35
	Beamwidth (º) along/athwartship	6.4/6.6	6.2/6.5	6.6/6.7	6.6/6.3	6.6/6.6	6.3/6.1	6.5/6.6	6.3/6.4	6.6/6.6
	Beam offset (º) along/athwartship	0.00/0.00	0.13/-0.04	0.04/-0.02	0.00/0.00	0.00/0.00	0.00/0.00	-0.00/0.00	0.00/0.00	0.00/0.00
	RMS deviation (dB)	0.13	0.18	0.10	0.10	0.10	0.21	0.10	0.14	0.25

120 kHz										
	Transducer peak gain (dB)	26.19	26.15	26.92	26.22	26.11	26.80	25.96	26.79	26.17
	Sa correction (dB)	-0.33	-0.29	-0.33	-0.39	-0.34	-0.38	-0.39	-0.35	–0.36
	Beamwidth (º) along/athwartship	6.3/6.5	6.1/6.2	6.4/6.5	6.5/6.4	6.5/6.6	6.0/6.0	6.4/6.6	6.1/6.4	6.5/6.6
	Beam offset (º) along/athwartship	0.00/0.00	-0.00/0.00	-0.00/0.00	0.00/0.00	-0.00/-0.00	0.00/0.00	-0.13/0.11	0.00/0.00	0.00/0.00
	RMS deviation (dB)	0.17	0.18	0.16	0.15	0.17	0.19	0.17	0.17	0.35
200 kHz										
	Transducer peak gain (dB)	24.92	25.10	24.90	25.27	25.31	25.16	25.25	25.35	24.96
	Sa correction (dB)	-0.17	-0.22	-0.27	-0.31	-0.24	-0.21	-0.29	-0.36	–0.25
	Beamwidth (º) along/athwartship	6.4/6.3	6.2/6.2	6.6/6.9	6.4/6.3	6.8/6.5	6.2/6.2	6.3/6.7	6.7/6.7	6.8/6.9
	Beam offset (º) along/athwartship	0.00/0.00	0.00/0.00	0.00/0.00	0.00/0.00	-0.27/-0.10	0.08/-0.08	0.00/0.00	0.00/0.00	0.00/0.00
	RMS deviation (dB)	0.19	0.18	0.20	0.20	0.21	0.18	0.21	0.18	0.39

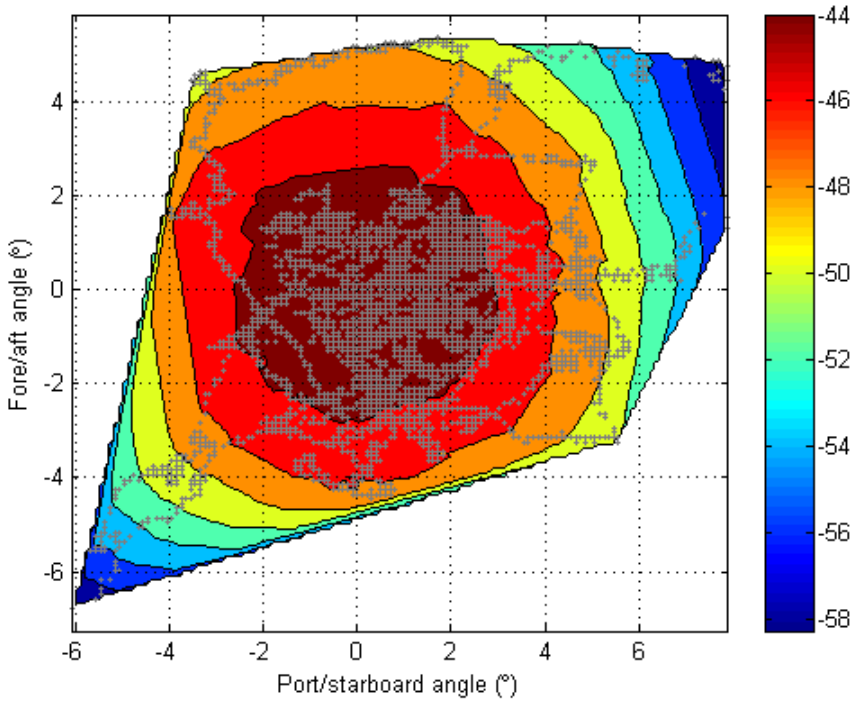

Figure A1.1: The 18 kHz estimated beam pattern from the sphere echo strength and position. The '+' symbols indicate where sphere echoes were received. The colours indicate the received sphere echo strength in dB re 1 m^2.

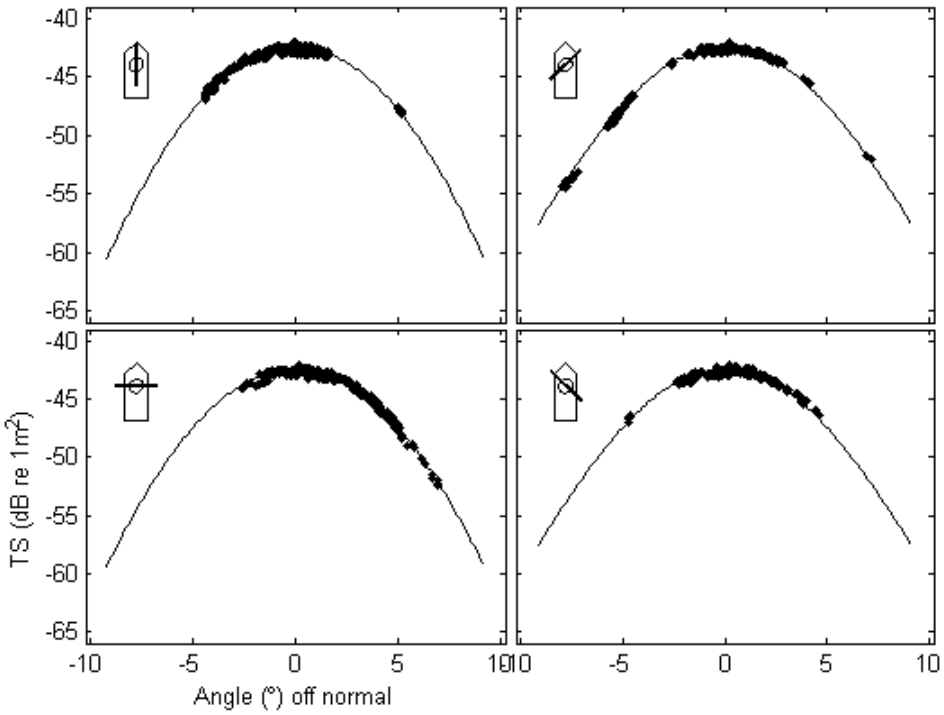

Figure A1.2: Beam pattern results from the 18 kHz analysis. The solid line is the ideal beam pattern fit to the sphere echoes for four slices through the beam.

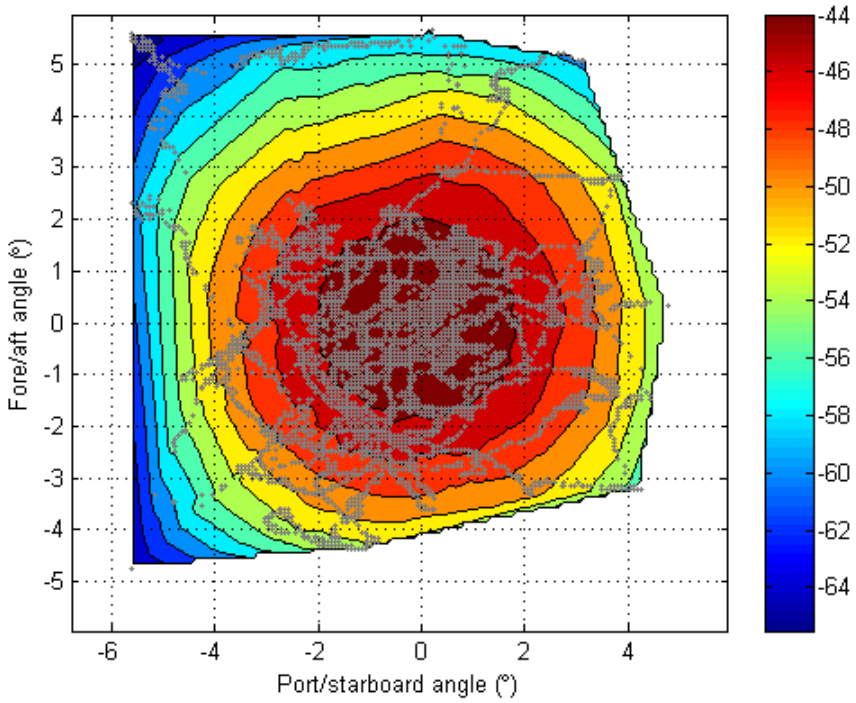

Figure A1.3: The 38 kHz estimated beam pattern from the sphere echo strength and position. The '+' symbols indicate where sphere echoes were received. The colours indicate the received sphere echo strength in dB re 1 m^2.

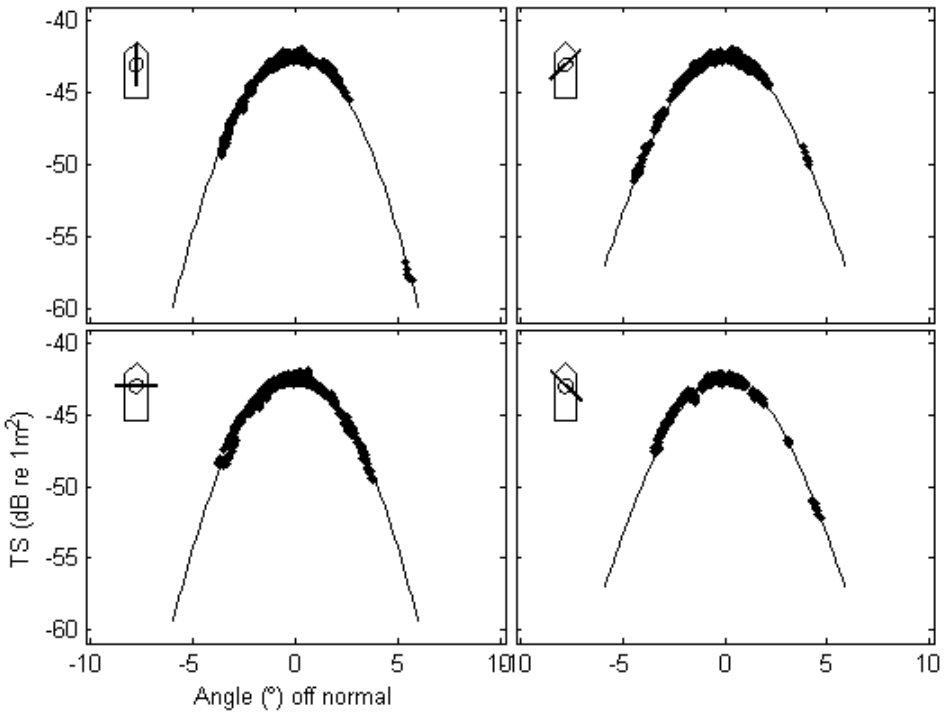

Figure A1.4: Beam pattern results from the 38 kHz analysis. The solid line is the ideal beam pattern fit to the sphere echoes for four slices through the beam.

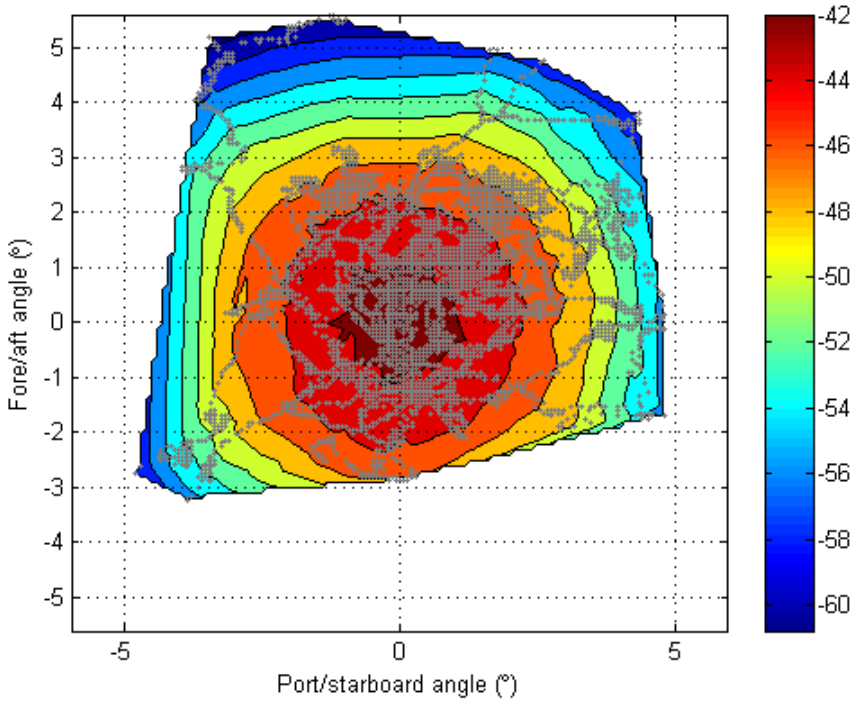

Figure A1.5: The 70 kHz estimated beam pattern from the sphere echo strength and position. The '+' symbols indicate where sphere echoes were received. The colours indicate the received sphere echo strength in dB re 1 m^2.

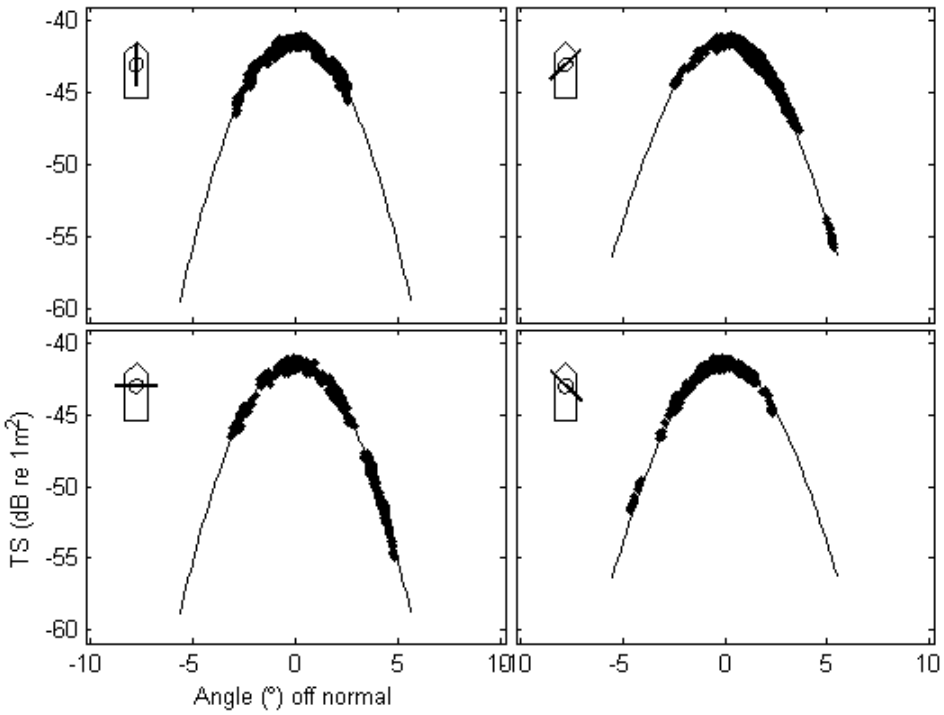

Figure A1.6: Beam pattern results from the 70 kHz analysis. The solid line is the ideal beam pattern fit to the sphere echoes for four slices through the beam.

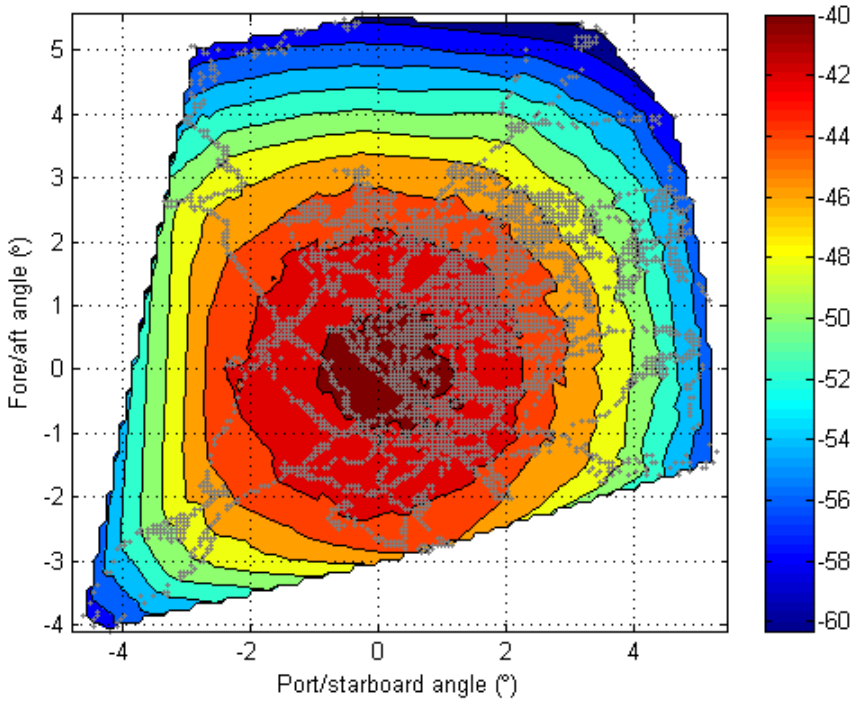

Figure A1.7: The 120 kHz estimated beam pattern from the sphere echo strength and position. The '+' symbols indicate where sphere echoes were received. The colours indicate the received sphere echo strength in dB re 1 m^2.

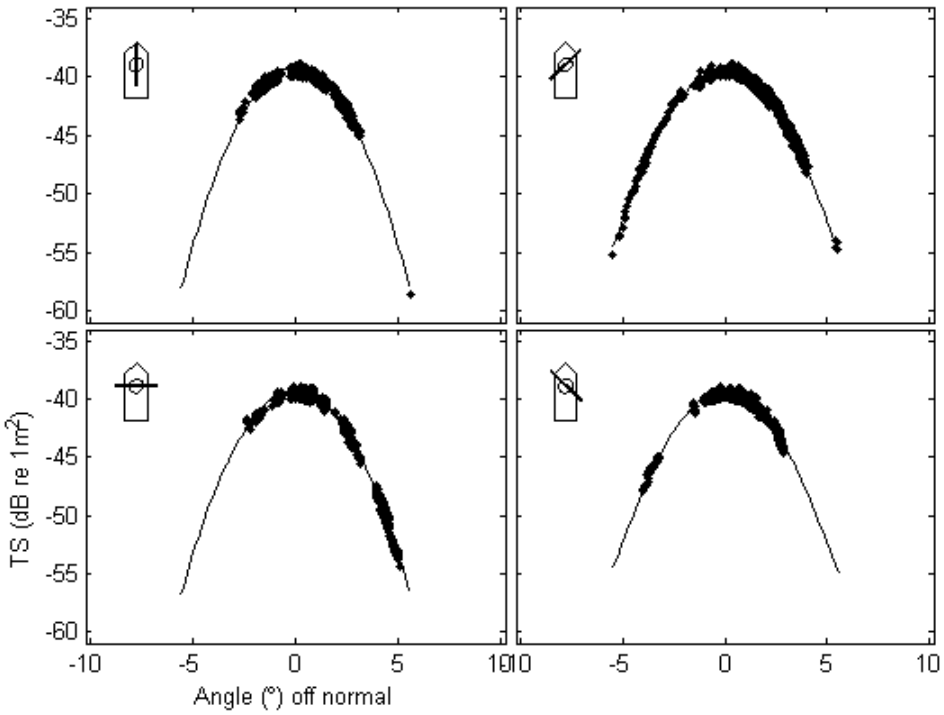

Figure A1.8: Beam pattern results from the 120 kHz analysis. The solid line is the ideal beam pattern fit to the sphere echoes for four slices through the beam.

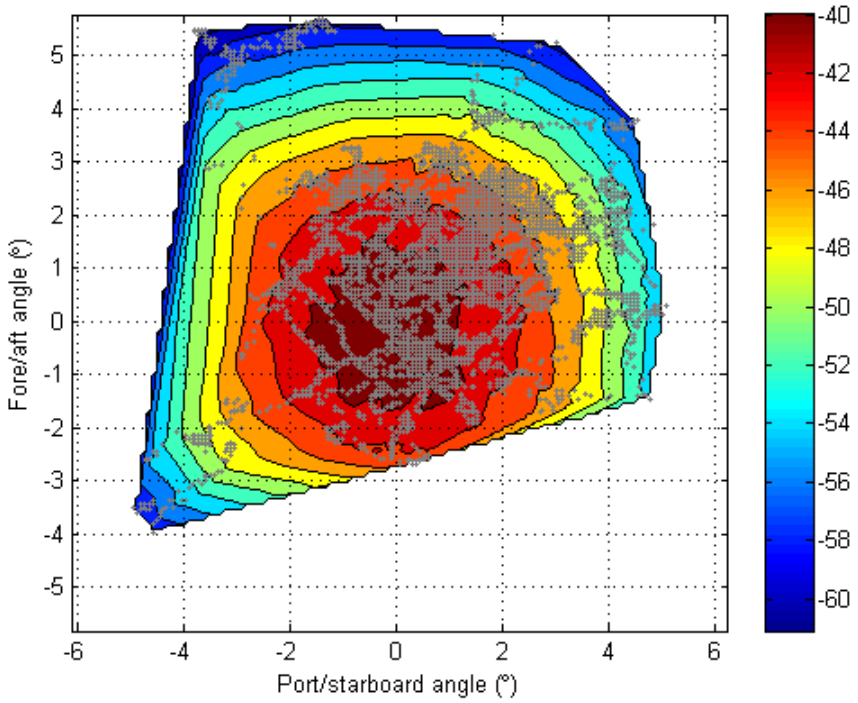

Figure A1.9: The 200 kHz estimated beam pattern from the sphere echo strength and position. The '+' symbols indicate where sphere echoes were received. The colours indicate the received sphere echo strength in dB re 1 m^2.

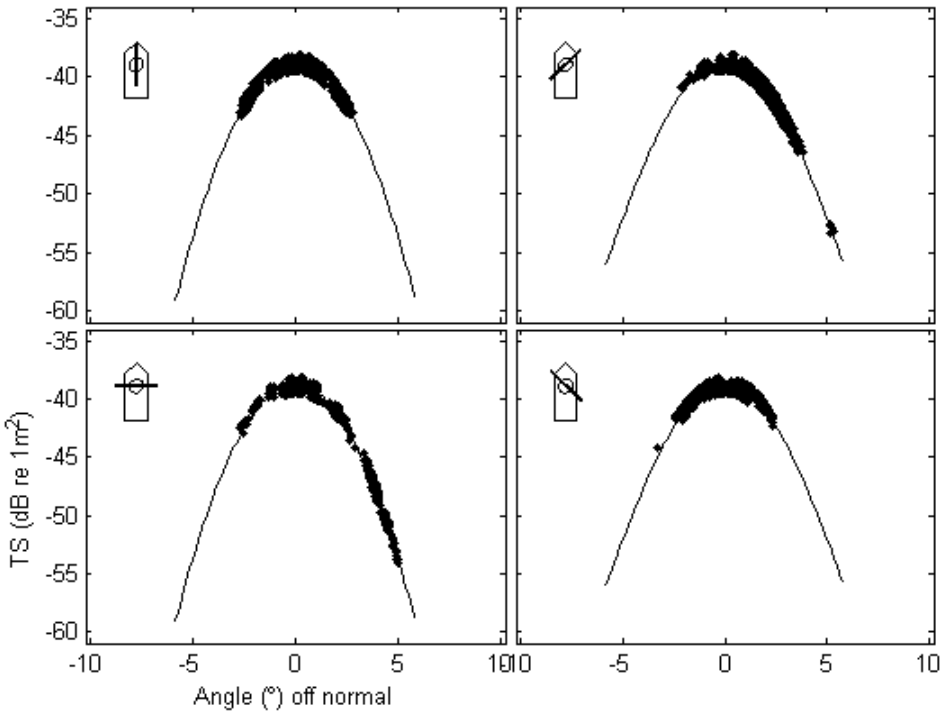

Figure A1.10: Beam pattern results from the 200 kHz analysis. The solid line is the ideal beam pattern fit to the sphere echoes for four slices through the beam.

APPENDIX 2: Towbody 4 calibration

Calibration of the Simrad EK60 echosounder in Towbody 4 took place on 27 August 2016 in East Bay, Marlborough Sounds (41˚ 09.4' S, 174˚ 20.1' E), at the start of the Campbell southern blue whiting acoustic survey (TAN1610), and in Perseverance Harbour, Campbell Island on 6 September (52˚ 33.03' S, 169˚ 09.89' E) and 7 September (52˚ 33.19' S, 169˚ 12.73' E), during the survey. The calibrations were conducted broadly according to the procedures in Demer et al. (2015). These were the first calibrations of the new EK60 echosounder in Towbody 4 (previously it was a CREST system).

In all calibrations, the towbody was lowered about 7 m below the surface, supported by the deployment wires and a nose rope to allow the pitch to be adjusted. A 38.1 mm tungsten carbide sphere was suspended by a single line about 15 m below the transducer. A weight was also deployed about 3 m below the sphere to steady the line. The transducer face, towbody window, sphere and associated lines were washed with a soap solution prior to entering the water in the Marlborough Sounds and in the second calibration at Campbell Island on 7 September, but this step was omitted on 6 September.

In the Marlborough Sounds, the weather during the calibration was improving, with 15–20 knots of westerly wind, no swell, and a 0.5 m chop. The vessel was anchored but swinging at 0.3–0.7 knots. Water depth was about 45 m. The towbody was put into the water at 09:45 NZST, but was run in passive mode while the hull echosounders were calibrated. The towbody calibration started at 11:57 and was completed at 13:09 NZST.

At Campbell Island on 6 September, the weather was fair with a 30 knot north-westerly wind and 1.0 m wind chop. The vessel was anchored in 30 m of water, but was swinging on the anchor at speeds up to 0.5 knots. Vessel motion was enough to move the towbody around the beam with little manipulation of the supporting lines. The calibration started at 14:16 and was completed at 16:45 NZST. On 7 September the wind was 35 knot southwest, with a 0.5 m chop. The anchorage was deeper (39 m), but the vessel was swinging faster than on 6 September (up to 1.2 knots), meaning the sphere was moving quickly through the beam. The calibration started at 08:56 and was completed at 12:14 NZST.

The echosounder was run from a PC (ER60-1) onboard *Tangaroa* and calibration data were saved into EK60 raw format files (tan1610-D20160826-T235708 on 27 August in the Marlborough Sounds, tan1610-D20160906-T021647 on 6 September, and tan1610-D20160906-T205627 and tan1610-D20160906-T215736 on 7 September at Campbell Island). Raw data are stored in the NIWA *acoustics* database. The EK60 transceiver settings in effect during the calibration are given in Table A2.1.

Temperature/salinity/depth profiles were taken using a Seabird SBE21 conductivity, temperature, and depth probe (CTD) during all calibrations. Estimates of acoustic absorption were calculated using the formulae in Doonan et al. (2003). Estimates of seawater sound speed and density were calculated using the formulae of Fofonoff & Millard (1983). The sphere target strength was calculated according to equations 6 to 9 in MacLennan (1981), using longitudinal and transverse sphere sound velocities of 6853 and 4171 m s^{-1} respectively and a sphere density of 14 900 kg m^{-3}.

Analysis

The data in the .raw EK60 file were extracted using custom-written software. The amplitude of the sphere echoes was obtained by filtering on range, and choosing the sample with the highest amplitude. The filter parameter *maxbBDiff1* which discarded sphere echoes which differed by more than 6 dB from the theoretical before estimating beam fit was increased to 9 dB because Towbody4 had very low values for sphere TS. Instances where the sphere echo was disturbed by fish echoes were discarded. The alongship and athwartship beam widths and offsets were calculated by fitting the sphere echo amplitudes to the Simrad theoretical beam pattern:

$$compensation = 6.0206\left(\left(\frac{2\theta_{fa}}{BW_{fa}}\right)^2 + \left(\frac{2\theta_{ps}}{BW_{ps}}\right)^2 - 0.18\left(\frac{2\theta_{fa}}{BW_{fa}}\right)^2\left(\frac{2\theta_{ps}}{BW_{ps}}\right)^2\right),$$

where θ_{ps} is the port/starboard echo angle, θ_{fa} the fore/aft echo angle, BW_{ps} the port/starboard beamwidth, BW_{fa} the fore/aft beamwidth, and *compensation* the value, in dB, to add to an uncompensated echo to yield the compensated echo value. The fitting was done using an unconstrained nonlinear optimisation (as implemented by the Matlab fminsearch function). The S_a correction was calculated from:

$$Sa, corr = 5\log 10\left(\frac{\sum P_i}{4P_{\max}}\right),$$

where P_i is sphere echo power measurements and P_{max} the maximum sphere echo power measurement. A value for $S_{a,corr}$ is calculated for all valid sphere echoes and the mean over all sphere echoes is used to determine the final $S_{a,corr}$.

Results

The results from the CTD casts are given in Table A2.2, along with estimates of the sphere target strength, sound speed, and acoustic absorption.

The calibration results are given in Table A2.3. The estimated beam pattern and sphere coverage are given in Figures A2.1–A2.4. The symmetrical nature of the pattern and the zero centre of the beam pattern indicate that the transducer and EK60 transceiver were operating correctly. The fits between the theoretical beam pattern and the sphere echoes is shown in Figure A2.4–A2.6, and confirm that the transducer beam pattern is correct.

The estimated peak gain (G_0) of 23.55 dB and the Sa correction of -0.51 dB in the Marlborough Sounds were estimated from 1302 sphere echoes within 0.21° of the beam centre (Table A2.3). This calibration was of excellent quality. The RMS of the difference between the Simrad beam model and the sphere echoes the sphere echoes out to 3.6° off axis was 0.05 dB (Table A2.3) - where <0.4 dB is satisfactory, <0.3 dB good, and <0.2 dB excellent. The first calibration at Campbell Island on 6 September suggested a sphere TS 1 dB lower than the calibration in the Marlborough Sounds, with an estimated G_0 of 23.02 dB from 751 on-axis echoes (Table A2.3). This large difference was unexpected, and we were also concerned about the variability in sphere echoes during this calibration (see Figure A2.5), even though the RMS deviation was not particularly high (0.20). When we repeated the calibration on 7 September, estimates were less variable (see Figure A2.6, RMS deviation = 0.11), and although the average on-axis sphere TS was lower than in the Marlborough Sounds, the difference was not large (0.3 dB) and might be explained by differences in water temperature (see Table A2.2). The estimated G_0 was 23.36 dB from 290 on-axis echoes, with a Sa correction of –0.45 dB (Table A2.3).

The G_0 values were all low compared to most hull-mounted ES38B transducers, and lower than those for Towbody 3 (G_0 24.34–24.67 in three calibrations in 2013–16, see Appendix 3). However, the first and third calibrations were consistent and of excellent quality. The results from the first calibration of Campbell Island on 6 September were anomalous and may have been caused by microbubbles due to our failure to soap the transducer face and towbody window.

Calibration coefficients estimated from the second Campbell Islands calibration (which was carried out in similar environmental conditions to those during the survey) were used for analysis of results from the Campbell Rise southern blue whiting survey (TAN1610).

Table A2.1: EK60 transceiver settings and other relevant parameters during the calibration.

Parameter	Value
Echosounder	Towbody 4 EK60
ER60 software version	2.4.3
Transducer model	ES38DD
Transducer serial number	28337
EK60 GPT serial number	009072069083
GPT software version	Not recorded
Sphere type/size	tungsten carbide/38.1 mm diameter
Operating frequency (kHz)	38
Towbody depth (m)	3
Transmit power (W)	2000
Pulse length (ms)	1.024
Transducer peak gain (dB)	26.5
Sa correction (dB)	0.0
Bandwidth (Hz)	2425
Sample interval (m)	0.192
Two-way beam angle (dB)	–20.60
Absorption coefficient (dB/km)	9.75
Speed of sound (m/s)	1500
Angle sensitivity (dB) alongship/athwartship	21.90/21.90
3 dB beamwidth (º) alongship/athwartship	7.10/7.10
Angle offset (º) alongship/athwartship	0.0/0.0

Table A2.2: Auxiliary calibration parameters derived from conductivity, temperature, depth measurements.

Parameter	Campbell Island 7 Sep	Campbell Island 6 Sep	Marlborough Sounds 27 Aug
Mean sphere range (m)	15.1	15.1	15.3
Mean temperature (ºC)	7.0	6.9	11.8
Mean salinity (psu)	34.3	34.4	35.0
Sound speed (m/s)	1478.2	1477.9	1496.4
Mean absorption (dB/km)	9.81	9.83	9.30
Sphere TS (dB re 1 m^2)	-42.34	–42.33	–42.41

Table A2.3: Echosounder calibration values. Transducer peak gain was estimated from mean sphere TS using Matlab calibration code version 7045.

Parameter	Campbell Island 7 Sep	Campbell Island 6 Sep	Marlborough Sounds 27 Aug
Mean TS within 0.21° of centre	-48.62	-49.29	-48.32
Std dev of TS within 0.21° of centre	0.09	0.33	0.06
Max TS within 0.21° of centre	-48.49	-48.64	-48.06
No. of echoes within 0.21° of centre	290	751	1 302
On axis TS from beam-fitting	-48.48	-49.37	-48.25
Transducer peak gain (dB)	23.36	23.02	23.54
Sa correction (dB)	-0.45	-0.51	-0.50
Beamwidth (º) alongship/athwarthship	7.09/7.09	7.37/7.32	7.22/7.32
Beam offset (º) alongship/athwarthship	0.00/0.00	-0.00/0.00	0.10/0.09
RMS deviation	0.11	0.20	0.05
Echoes used to estimate the beam shape	31 555	23 068	14 492

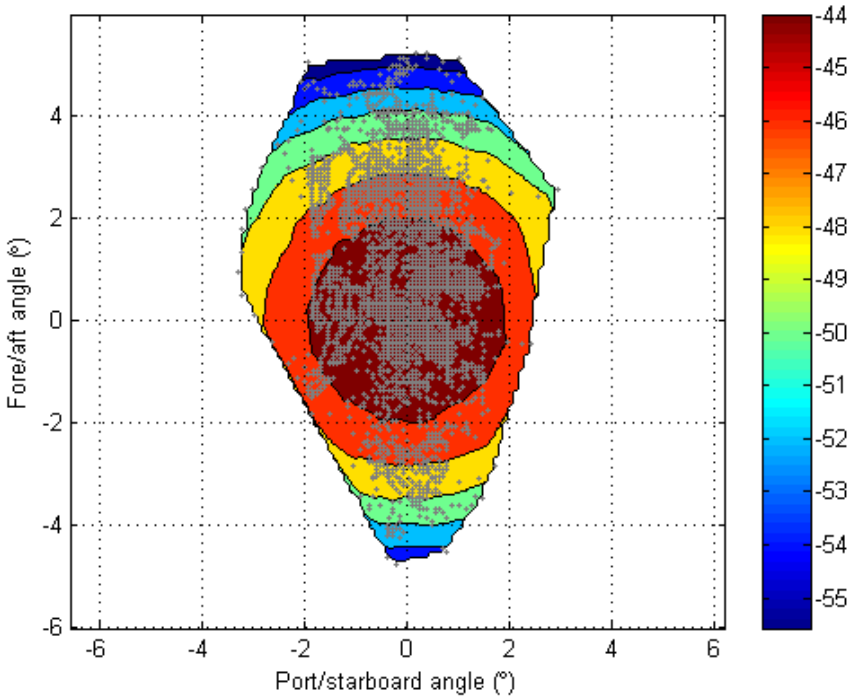

Figure A2.1: The estimated beam pattern from the sphere echo strength and position for the calibration in the Marlborough Sounds. The '+' symbols indicate where sphere echoes were received. The colours indicate the received sphere echo strength in dB re 1 m^2.

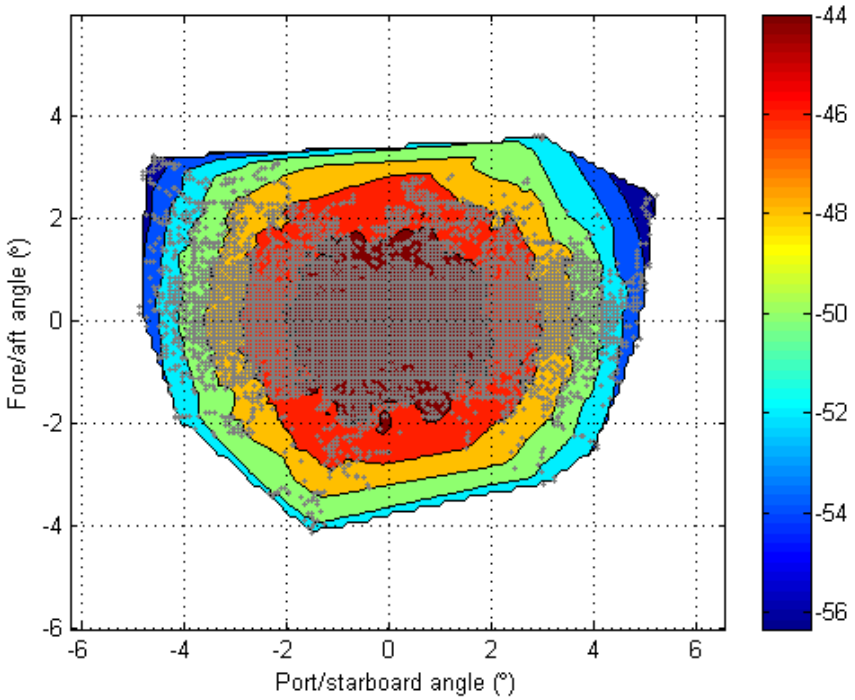

Figure A2.2: The estimated beam pattern from the sphere echo strength and position for the calibration at Campbell Island on 6 September. The '+' symbols indicate where sphere echoes were received. The colours indicate the received sphere echo strength in dB re 1 m^2.

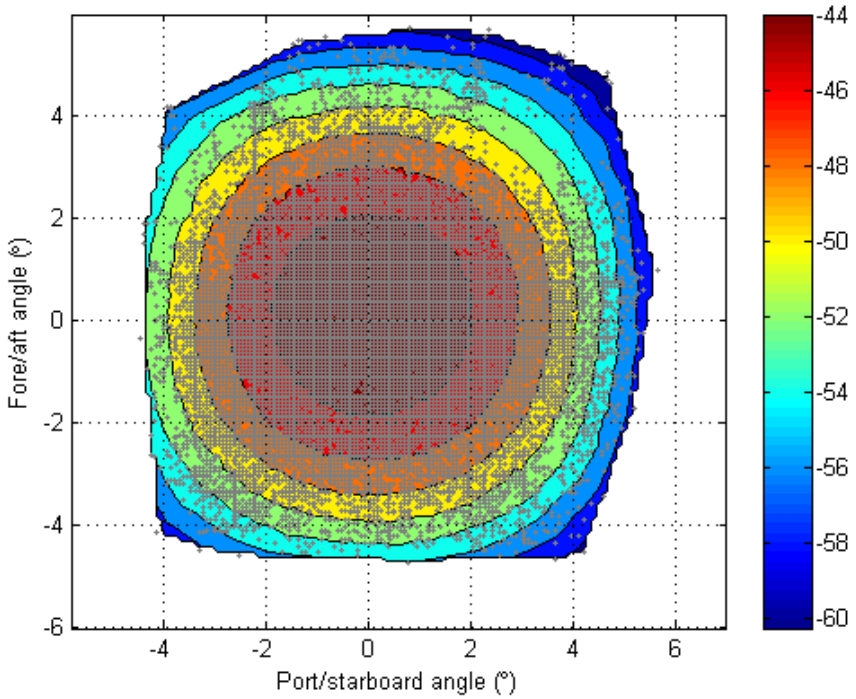

Figure A2.3: The estimated beam pattern from the sphere echo strength and position for the calibration at Campbell Island on 7 September. The '+' symbols indicate where sphere echoes were received. The colours indicate the received sphere echo strength in dB re 1 m^2.

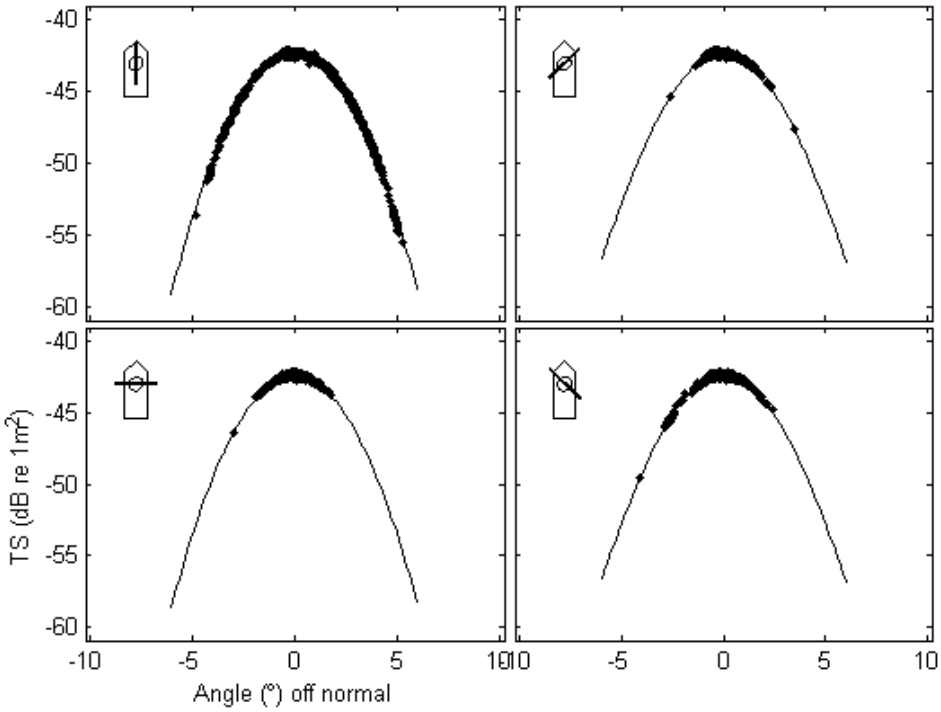

Figure A2.4: Beam pattern results from the calibration analysis for the Marlborough Sounds. The solid line is the theoretical beam pattern fit to the sphere echoes for four slices through the beam.

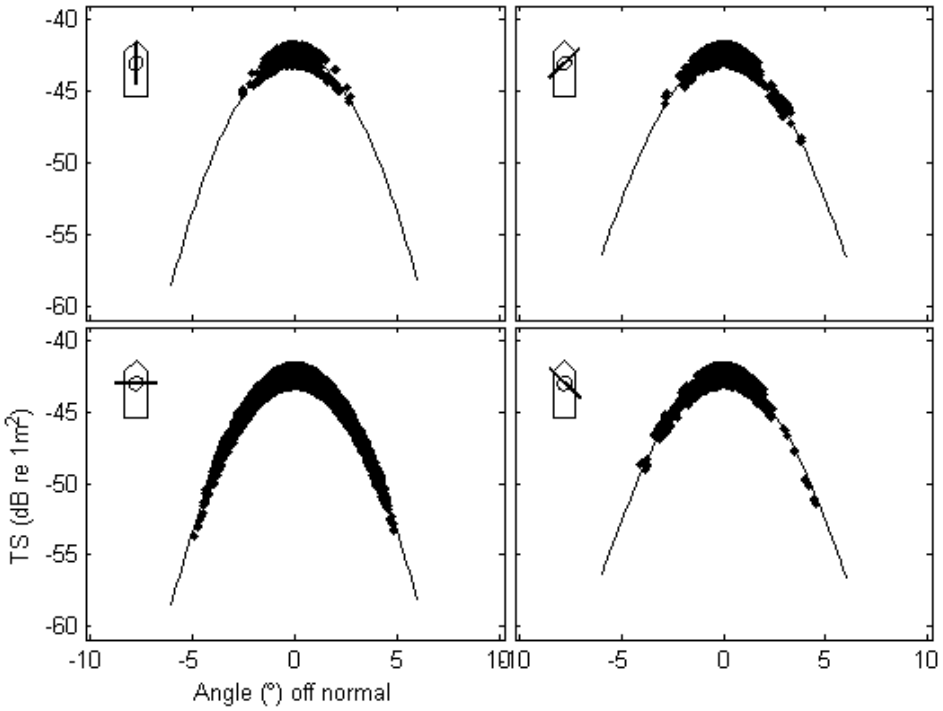

Figure A2.5: Beam pattern results from the calibration analysis for Campbell Island on 6 September. The solid line is the theoretical beam pattern fit to the sphere echoes for four slices through the beam.

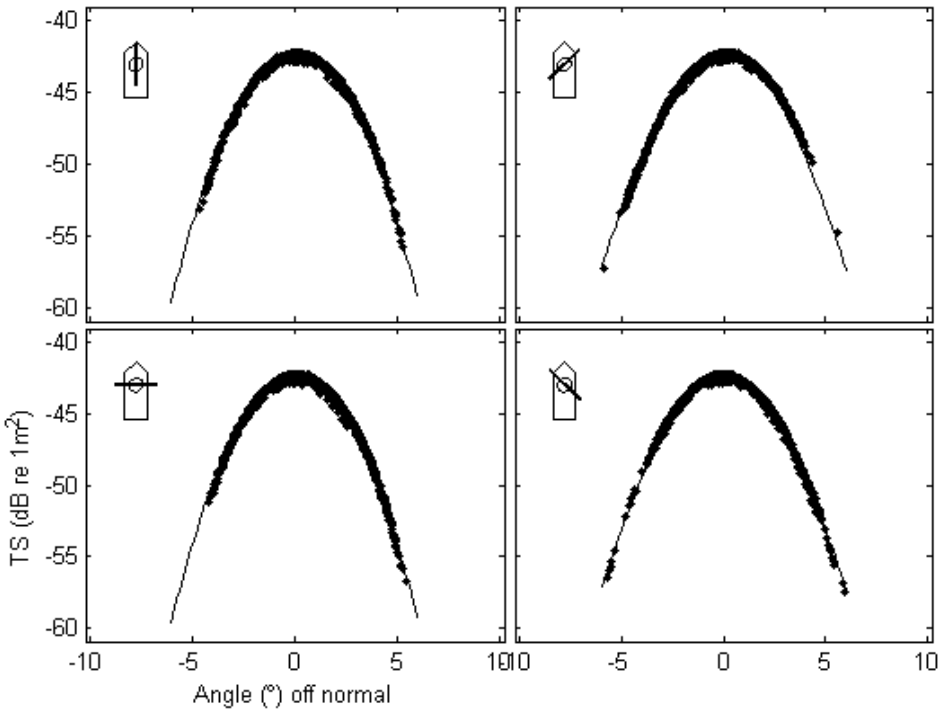

Figure A2.6: Beam pattern results from the calibration analysis for Campbell Island on 7 September. The solid line is the theoretical beam pattern fit to the sphere echoes for four slices through the beam.

APPENDIX 3: Towbody 3 calibration.

Calibration of the Simrad EK60 echosounder in Towbody 3 took place in Perseverance Harbour, Campbell Island (52˚ 33.03' S, 169˚ 09.89' E) on 6 September 2016, in the middle of the acoustic survey of spawning southern blue whiting on the Campbell Island Rise (TAN1610). This was the third at-sea calibration of the EK60 echosounder in Towbody 3 (previously it was a CREST system). The previous two calibrations were in 2013.

The calibration started at 10:30 NZST. The towbody was lowered about 7 m below the surface, supported by the deployment wires and a nose rope to allow the pitch to be adjusted. A 38.1 mm tungsten carbide sphere was suspended by a single line about 15 m below the transducer. A weight was also deployed about 3 m below the sphere to steady the line. The transducer face, towbody window, sphere and associated lines were washed with a soap solution prior to entering the water.

The weather was fair with a 30 knot north-westerly wind and 1.0 m wind chop. The vessel was anchored in 30 m of water, but was swinging on the anchor at speeds up to 0.5 knots. Vessel motion was enough to move the towbody around the beam with little manipulation of the supporting lines. The echosounder was run from a PC (ER60-1) onboard *Tangaroa* and calibration data were saved into one EK60 raw format file (tan1610-D20160905-T223146). Raw data are stored in the NIWA *acoustics* database. The EK60 transceiver settings in effect during the calibration are given in Table A3.1. The calibration was completed at 12:21 NZST.

A temperature/salinity/depth profile was taken using a Seabird SBE21 conductivity, temperature, and depth probe (CTD). Estimates of acoustic absorption were calculated using the formulae in Doonan et al. (2003). Estimates of seawater sound speed and density were calculated using the formulae of Fofonoff & Millard (1983). The sphere target strength was calculated according to equations 6 to 9 in MacLennan (1981), using longitudinal and transverse sphere sound velocities of 6853 and 4171 m s^{-1} respectively and a sphere density of 14 900 kg m^{-3}.

Analysis

The data in the .raw EK60 files were extracted using custom-written software (version 7045). The amplitude of the sphere echoes was obtained by filtering on range, and choosing the sample with the highest amplitude. Instances where the sphere echo was disturbed by fish echoes were discarded. The alongship and athwartship beam widths and offsets were calculated by fitting the sphere echo amplitudes to the Simrad theoretical beam pattern:

$$compensation = 6.0206\left(\left(\frac{2\theta_{fa}}{BW_{fa}}\right)^2 + \left(\frac{2\theta_{ps}}{BW_{ps}}\right)^2 - 0.18\left(\frac{2\theta_{fa}}{BW_{fa}}\right)^2\left(\frac{2\theta_{ps}}{BW_{ps}}\right)^2\right),$$

where θ_{ps} is the port/starboard echo angle, θ_{fa} the fore/aft echo angle, BW_{ps} the port/starboard beamwidth, BW_{fa} the fore/aft beamwidth, and *compensation* the value, in dB, to add to an uncompensated echo to yield the compensated echo value. The fitting was done using an unconstrained nonlinear optimisation (as implemented by the Matlab fminsearch function). The S_a correction was calculated from:

$$Sa, corr = 5\log 10\left(\frac{\sum P_i}{4P_{\max}}\right),$$

where P_i is sphere echo power measurements and P_{max} the maximum sphere echo power measurement. A value for $S_{a,corr}$ is calculated for all valid sphere echoes and the mean over all sphere echoes is used to determine the final $S_{a,corr}$.

Results

The results from the CTD cast are given in Table A3.2, along with estimates of the sphere target strength, sound speed, and acoustic absorption.

The calibration results are given in Table A3.3. The estimated beam pattern and sphere coverage are given in Figure A3.1. The symmetrical nature of the pattern and the zero centre of the beam pattern indicate that the transducer and EK60 transceiver were operating correctly. The fits between the theoretical beam pattern and the sphere echoes is shown in Figure A3.2 and confirms that the transducer beam pattern is correct. The estimated peak gain (G_0) of 24.61 dB and the Sa correction of -0.56 dB were estimated from 263 sphere echoes within 0.21° of the beam centre (Table A3.3). The G_0 value was close (0.08 dB lower) to that from the first calibration in 2013, but about 0.27 dB higher than the value from the second calibration (Table A3.3). The linear difference between the two calibrations in 2013 was about 11%, which was higher than expected. The RMS of the difference between the Simrad beam model and the sphere echoes out to 3.6° off axis was 0.11 dB (Table A3.3), indicating that the 2016 calibration was of excellent quality (<0.4 dB is acceptable, <0.3 dB good, and <0.2 dB excellent).

Table A3.1: EK60 transceiver settings and other relevant parameters during the calibration.

Parameter	Value
Echosounder	Towbody 3 EK60
ER60 software version	2.4.3
Transducer model	ES38DD
Transducer serial number	28332B
EK60 GPT serial number	009072069o87
GPT software version	Not recorded
Sphere type/size	tungsten carbide/38.1 mm diameter
Operating frequency (kHz)	38
Towbody depth (m)	3
Transmit power (W)	2000
Pulse length (ms)	1.024
Transducer peak gain (dB)	26.5
Sa correction (dB)	0.0
Bandwidth (Hz)	2425
Sample interval (m)	0.192
Two-way beam angle (dB)	–20.60
Absorption coefficient (dB/km)	9.75
Speed of sound (m/s)	1500
Angle sensitivity (dB) alongship/athwartship	21.90/21.90
3 dB beamwidth (º) alongship/athwartship	7.10/7.10
Angle offset (º) alongship/athwartship	0.0/0.0

Table A3.2: Auxiliary calibration parameters derived from conductivity, temperature, depth measurements.

Parameter	Value
Mean sphere range (m)	15.3
Mean temperature (ºC)	6.9
Mean salinity (psu)	34.4
Sound speed (m/s)	1477.9
Mean absorption (dB/km)	9.83
Sphere TS (dB re 1 m^2)	–42.33

Table A3.3: Echosounder calibration values for the three at-sea calibrations of Towbody 3. Transducer peak gain was estimated from mean sphere TS using Matlab calibration code

Parameter	Sep 16	Sep 13	July 13
Mean TS within 0.21° of centre	-46.11	-46.65	-46.04
Std dev of TS within 0.21° of centre	0.15	0.16	0.12
Max TS within 0.21° of centre	-45.44	-46.45	-45.86
No. of echoes within 0.21° of centre	263	57	124
On axis TS from beam-fitting	-45.97	-46.50	-46.02
Transducer peak gain (dB)	24.61	24.34	24.69
Sa correction (dB)	-0.56	-0.57	-0.69
Beamwidth (º) alongship/athwarthship	7.06/6.92	7.00/6.95	7.09/7.13
Beam offset (º) alongship/athwarthship	0.00/0.00	0.08/0.03	0.10/-0.02
RMS deviation	0.11	0.11	0.08
Echoes used to estimate the beam shape	21 102	23 886	9 460

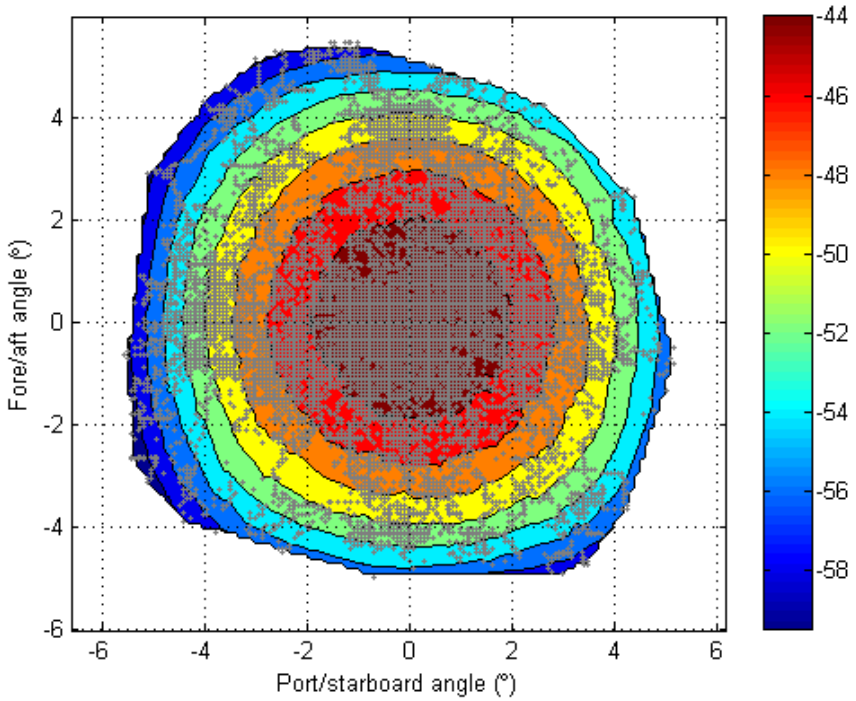

Figure A3.1: The estimated beam pattern from the sphere echo strength and position for the calibration. The '+' symbols indicate where sphere echoes were received. The colours indicate the received sphere echo strength in dB re 1 m^2.

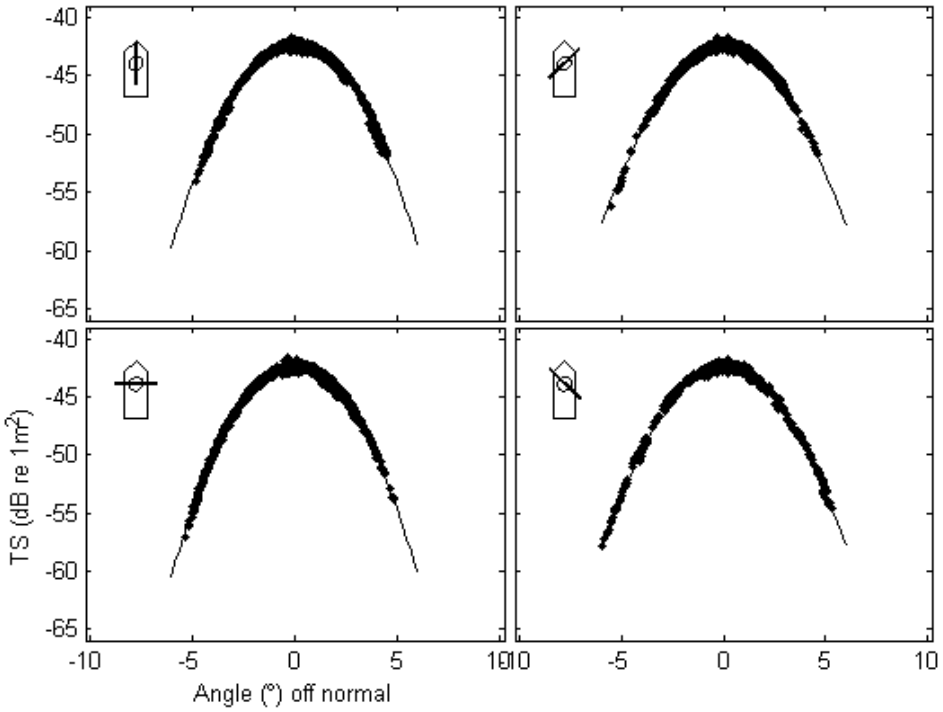

Figure A3.2: Beam pattern results from the calibration analysis. The solid line is the theoretical beam pattern fit to the sphere echoes for four slices through the beam.

APPENDIX 4: Description of gonad development used for staging SBW

Research gonad stage		Males	Females
1	Immature	Testes small and translucent, threadlike or narrow membranes.	Ovaries small and translucent. No developing oocytes.
2	Resting	Testes thin and flabby; white or transparent.	Ovaries are developed, but no developing eggs are visible.
3	Ripening	Testes firm and well developed, but no milt is present.	Ovaries contain visible developing eggs, but no hyaline eggs present.
4	Ripe	Testes large, well developed; milt is present and flows when testis is cut, but not when body is squeezed.	Some or all eggs are hyaline, but eggs are not extruded when body is squeezed.
5	Running-ripe	Testis is large, well formed; milt flows easily under pressure on the body.	Eggs flow freely from the ovary when it is cut or the body is pressed.
6	Partially spent	Testis somewhat flabby and may be slightly bloodshot, but milt still flows freely under pressure on the body.	Ovary partially deflated, often bloodshot. Some hyaline and ovulated eggs present and flowing from a cut ovary or when the body is squeezed.
7	Spent	Testis is flabby and bloodshot. No milt in most of testis, but there may be some remaining near the lumen. Milt not easily expressed even when present.	Ovary bloodshot; ovary wall may appear thick and white. Some residual ovulated eggs may still remain but will not flow when body is squeezed.

APPENDIX 5: Calculation of sound absorption coefficients

The Seabird SM-37 Microcat CTD datalogger was mounted on the headline of the net during 19 bottom trawls to determine the absorption coefficient and speed of sound, and to define water mass characteristics in the area. Average sound absorption was estimated using the formula of Doonan et al. (2003) (Table A5.1). The average absorption estimate of 9.44 dB km^{-1} was used when estimating SBW biomass (see Section 3.6).

Table A5.1: Estimates of acoustic absorption (at 38 kHz) for the Campbell Island Rise acoustic survey area in 2016. Absorption was calculated from CTD profiles made during the survey using the formula of Doonan et al. (2003).

Station number	Max depth (m)	Mean temperature (˚C)	Mean salinity (PSU))	Absorption (dB km^{-1})
1	450	7.20	34.39	9.41
2	403	7.21	34.39	9.46
3	386	7.25	34.39	9.53
4	486	7.18	34.39	9.40
5	509	7.22	34.39	9.49
6	508	7.28	34.39	9.40
7	361	7.43	34.42	9.41
10	348	7.44	34.41	9.49
11	417	7.37	34.41	9.37
13	459	7.20	34.39	9.38
15	413	7.33	34.40	9.48
16	416	7.24	34.39	9.40
17	344	7.30	34.40	9.51
18	356	7.21	34.39	9.46
20	416	7.23	34.39	9.40
21	418	7.23	34.39	9.46
22	467	7.20	34.39	9.40
23	319	7.17	34.38	9.50
25	431	7.23	34.39	9.43
Average	509	7.26	34.39	9.44